universität wien

Masterarbeit / MASTER'S THESIS

Titel der Masterarbeit / Title of the Master's Thesis

„Statistical analysis of the distribution of the different cell cycle phases of different cell cultures via LA-ICP-TOFMS“

verfasst von / submitted by

Claude Molitor

angestrebter akademischer Grad / in partial fulfilment of the requirements for the degree of

Master of Science (MSc)

Wien, 2022 / Vienna 2022

Studienkennzahl lt. Studienblatt / degree programme code as it appears on the student record sheet:	UA 066 862
Studienrichtung lt. Studienblatt / degree programme as it appears on the student record sheet:	Masterstudium Chemie
Betreut von / Supervisor:	Univ.-Prof. Dr. Gunda Köllensperger
Mitbetreut von / Co-Supervisor:	Mag. Dr. Sarah Theiner

This work has been executed from the 07.11.21 until the 31.11.22 in the lab of Univ.-Prof. Dr. Gunda Köllensperger (Institute of Analytical Chemistry, University of Vienna) under the co-supervision of Dr. Sarah Theiner.

Acknowledgment

First of all, I would like to thank Pr. Dr. Koellensperger for enabling me to do my master thesis within her working group and a lot of information and knowledge she shared with me. Furthermore, I want to show my gratitude letting me join all of seminars as well as the possibility to present my master thesis on the Junganalytikerforum. I would also like to thank Dr. Sarah Theiner for being the secondary corrector of my master thesis as well as for being my co-supervisor.

Lots of gratitude appertains to Anna Schoeberl for her help during theoretical and practical part of the master thesis, giving me the possibility to always ask question and help me in case of problems which occurred. Also, gratitude to Gabriel Braun for the help with the segmentation because without him, this master thesis would not have worked out too. I wish both all the best for their future projects and their attainment of their PhD-title.

I would also like to thank the whole Koellensperger lab in general for their help and kindness to include me that well into their group and the ideas their brought to light to help me out.

Furthermore, I want to thank Univ.-Prov. Dr. Walter Berger and his working group, especially Petra Vician, all from the Medical University of Vienna, for all their expertise, help and the work they put into the cell cultivation. There is no better cooperation partner I could imagine.

And lastly, I want to thank my family and friends for supporting me in every manner they could do during the master thesis.

universität wien

Philologisch-Kulturwissenschaftliche Fakultät
Institut für Germanistik
Universitätsring 1
A-1010 Wien

http://spl-germanistik.univie.ac.at/

Eidesstattliche Erklärung im Rahmen von schriftlichen Arbeiten

Angaben zur Studierenden / zum Studierenden	
Matrikelnummer:	11931997
Zuname:	Molitor
Vorname(n):	Claude
Studienkennzahl (Beispiel: A 066 817):	UA 066 862

Erklärung

Ich erkläre eidesstattlich, dass ich die Arbeit selbständig angefertigt, keine anderen als die angegebenen Hilfsmittel benutzt und alle aus ungedruckten Quellen, gedruckter Literatur oder aus dem Internet im Wortlaut oder im wesentlichen Inhalt übernommenen Formulierungen und Konzepte gemäß den Richtlinien wissenschaftlicher Arbeiten zitiert, durch Fußnoten gekennzeichnet bzw. mit genauer Quellenangabe kenntlich gemacht habe.

31.11.22

Datum | Unterschrift der / des Studierenden

HINWEIS: **Diese Erklärung ist für wissenschaftliche Arbeiten, die im Rahmen von Proseminaren, Seminaren und anderen prüfungsimmanenten Lehrveranstaltungen erstellt werden, verbindlich auszufüllen und den Arbeiten beizulegen.**

Table of contents

I List of figures

II List of tables

III List of Schemes

IV List of Appendix

V List of Abbreviations

cyclin dependent kinase = CDK

CDK inhibitors = CKI

Cisplatin treated sample = cis

Control sample = ctr

deoxyribonucleic acid = DNA

gap phase 1 = G1

gap phase 2 = G2

ground state = G0

interphase = I

iodo-desoxy-uridine = IdU

maleimido-mono-amide-DOTA = mDOTA

mitosis = M

phosphorylated retinoblastoma = pRb

retinoblastoma = Rb

taxol treated sample = tax

Tri buffered saline = TBS

0% serum sample = ser

Abstract

In this work we developed an analytical method for the determination of the different cell cycle phases of different cell cultures in form of cytospins. The samples consisted of cells which were deposited on glass slides via cytospin technology. Aim of the work was to dissect the role of cell cycle in metal-based drug mode of action via single cell analysis based on mass cytometry. For this, the cells were treated with different methods to arrest the cells in different cell cycle phases in order to analyze different compositions. The main method used for the visualization of the cell cycle phases is laser ablation in combination with inductively coupled plasma time-of-flight mass spectrometry (LA-ICP-TOFMS). Beforehand, an adequate sample preparation has been set up and optimized for the staining with metal labeled antibodies and markers in order to be able to visualize the fours cell cycle phases as well as the DNA. In cooperation with a bioinformation, four segmentation methods have been tested and pipelines have been set up for the optimal segmentation of the cytospins. This data and method enables a fast and easy statistical evaluation of a defined cell population according to their cell cycle phase that they are in with R. The method will serve for screening cellular metal-based candidate drugs accumulation with regard to cell cycle.

Zusammenfassung

In dieser Arbeit wurde eine analytische Methode zur Bestimmung der verschiedenen Zellzyklusphasen von Zelllinien entwickelt. Die Proben bestanden aus Zellen die mittels Cytospin-Technlogie auf Oberflächen deponiert wurden. Ziel der Methode war es die intrazelluläre Akkumulation metallhaltiger Zytostatika in Bezug auf den Zellzyklus zu untersuchen. Hierfür wurden Krebszellen und Epithelzellen in Modellversuchen so kultibiert, dass sie in verschiedenen Zellzyklusphasen angehalten wurden. Die so erhaltenen unterschiedliche Zellzyklusphasenzusammensetzungen konnten analysiert werden. Die eigentliche Analyse und Visualisierung der Zellzyklusphasen wurde mittels Laser ablation in Kombination mit induktiv gekoppelter Plasma time-of-flight Massenspektrometrie (LA-ICP-TOFMS) erreicht. Dazu musste eine geeignete Probenvorbereitung entwickelt und optimiert werden, um die verschiedenen Zellzyklusphasen zu markieren. Hierfür wurden die Zellen einerseits mit IdU inkubiert, andererseits wurden die auf den Cytospins fixierten Zellen mit unterschiedlichen Metall-markierten Antikörpern versetzt, die für die unterschiedlichen Zellzyklusphasen spezifische Proteine binden und so nachher zur Erkennung der

Zellzyklusphasen dienen. Bei diesem Schritt wurden noch zwei weitere Marker verwendet, die einerseits die DNA, als auch die proliferierenden Zellen erkennbar machten, um so eine Zellsegmentierung zu ermöglichen. Ein wichtiger Teil der Masterarbeit bestand darin die Methode zur Zellsegmentierung zu optimieren und eine statistische Auswertung zur Bestimmung der verschiedenen Zellzyklusphasen mittels R zu entwickeln.

1. Introduction

Mass cytometry is the combination between two disciplines. The aim is to gather as much information as possible from complex cellular systems and processes (cytometry) via time-of-flight mass spectrometry in combination with an inductively coupled plasma source (ICP-TOFMS) (mass). Cancer cells or the cell population in a tumor are very heterogeneous when it comes to the genetic information, the metabolome, the proteome but also their behavior within their environment[1]. For this reason, single cell analysis become more and more important to differentiate between the different cells within one population and thus learning more from the complex connections of the matrix's components. One other technique is flow cytometry, where proteins are tagged with fluorochrome conjugated antibodies within a cell, also named fluorophores. Here, the cells being in suspension are passing one by one through a laser beam which excites the fluorophores within the cell. The excited fluorophores remit light with a different wavelength which is measured. By using different types of fluorophores, different wavelengths can be reemitted and thus several proteins can be tracked down. The emitted wavelengths however do not give narrow bands but rather broader bands which can slightly overlap other wavelengths and thus limit the number of possible fluorophores used within one measurement. The intrinsic size of the cells as well as the granularity of the cell can be measured by the principle of light scattering.[2] As the method of choice in mass cytometry is mass spectrometry, it can easily be differentiated between different isotopes of elements as the resolution of the mass to charge ratios measured are more distinct compared to the broad bands measured in flow cytometry which leads to a fluorescence overlap.[3] This is enabled by different sorts of tagged molecules such as metal labeled antibodies, intercalators (especially DNA-intercalators) or modified nucleotides which are getting incorporated into the cell such as iodo-desoxy-uridine (IdU).[4] This combination of markers has already been used to investigate the cell cycle phases by single cell mass cytometry.[4-5] The three types of tagging molecules are explained further on page 20. Up to now, it is already possible to track over 40 parameters within one measurement to gather information about cancer immune microenvironments via imaging mass cytometry.[6]

For single cell mass cytometry, cells in a suspension are lead one by one into the ICP-TOFMS to be analyzed. Thus, the goal is to specifically track down proteins or other cell compartments by tagging them with enantiomerically pure metals or elements.

In this work, we focused on imaging mass cytometry with the aim of establishing methods for cell cycle analysis. The overall goal in the future is to link cell cycle data of single cells to metal

based drug accumulation. The instrumentation used is laser ablation in combination with inductively coupled plasma time-of-flight mass spectrometry (LA-ICP-TOFMS). The cytospins are placed into a cobalt ablation chamber and are set under a vacuum. A laser beam (Teledyne Ir laser) ablates the sample spot by spot and each ablated part of the sample is lead via a helium flow into the ICP-torch where it is vaporized, atomized, and ionized within an argon plasma. The ions are discriminated and measured within an TOFMS (TOFWERK AG). For every lasershot, the intensities for each mass to charge ratio from 12 to 256 are measured. The lasershots combined will get an image where each ablated spot represents a pixel within an image. Thus, LA-ICP-TOFMS is a visualization method where the distribution of different mass to charge ratios can be seen and can be used for single cell analysis by segmenting the cells based on the image received. From the segmented area, other signals such as the used metal labeled antibodies can be measured and used for the evaluation. A collision gas consisting of He and H_2 has been used to tune and increase the sensitivity of higher mass elements, as most metals from the markers will have higher masses which improves the usability of the raw data received.

The samples getting analyzed are cytospins which has been made by the Medical University of Vienna (working group of Univ.-Prof. Dr. Berger). Two different cell lines have been used, the A2780 human ovarian cancer cell line and the HaCaT cell line which are healthy but aneuploid and immortalized human keratinocytes. In a first try, the cancer cells have been used, as cancer cells have a disturbed cell cycle homeostasis, and they are most of the time in a proliferating state. Furthermore, one potential usage of this work would be to better understand other problems/questions regarding cancer research by implementing information about the cell cycle phases into their work simply by using four more markers. In special, the aim is to dissect the role of cell cycle in metal-based drug mode of action via single cell analysis based on mass cytometry. Honghzhe Sun et al has for example found a positive correlation among the intracellular arsenic contents, the ratios of apoptosis and death cells.[7] This work should also enable to learn more about the basis of more effective metal based drugs (arsenic or platinum based for example) connected to the cell cycle phases and thus provide more effective drug development.

Therefore, developing a procedure on the potential future biological matrix would be of great interest and cancer cells being proliferating cells seem to be the optimal samples for the analysis of the four cell cycle phases. However, key mechanisms can be disturbed in cancer cells as there can be many reasons for cells to become cancer cells. It must be considered that when

tagging special proteins characteristic for the progression of the cell cycle phases that they might not be present or functional within cancer cells.[8] If his would be the case, it would be easier to develop a protocol based on healthy cells where the cell cycle is not disturbed.

The cell cycle is divided into two major cell cycle states, the interphase (I) and miotic phase which consists of the mitosis (M-phase). The interphase can be subdivided into the two gap phases G1 and G2, as well as the synthetic phase S. The mitosis can be subdivided into the prophase, metaphase, anaphase and telophase which are not differentiated within this work, but rather between the actual cell cycle phases G1, S, G2 and M. Cells which are not proliferating are in the so-called ground state (G0).[9] Most cells in organisms are in this state[9-10], whereas most of the cells analyzed within this work will not be in the ground state but ideally in one of the four cell cycle phases as later explained.

The cell cycle is a very complex sequence of internal and external events which lead to the progression or the maintenance in the different cell cycle phases. The beginning of the cell cycle is initiated by the progression from the non-proliferating cells in the G0 ground state into the first gap phase G1. This mainly depends on external stimuli like growth factors and mitogens.[9-10] The progression from one cell cycle phases into the next phase however mainly depends on internal stimuli.[10] Most important for the progression of the cell cycle phases are the so-called cyclins by interacting with their respective cyclin dependent kinases (CDK). The cyclins are the regulatory unit which bind to the CDKs whereas the CDKs are the catalytic partner which finally enables the phosphorylation, the activity of the enzyme.[10-11] The interaction and formation of cyclins and CDK-complexes are for example crucial for the phosphorylation of different proteins necessary for the DNA synthesis (late G1 and S) or the formation of structural components (late G2 and M) which are necessary for the mitosis.[9-10] Scheme 1 and Scheme 2 provide an overview of the cell cycle phases and the main cyclins as well as CDKs implemented into the cell cycle progression.[11] This scheme however is just a simplification of the cell cycle as many more mechanisms and signaling pathways are implemented and the boundaries between the different cell cycle phases are a smooth transition rather than defined events.

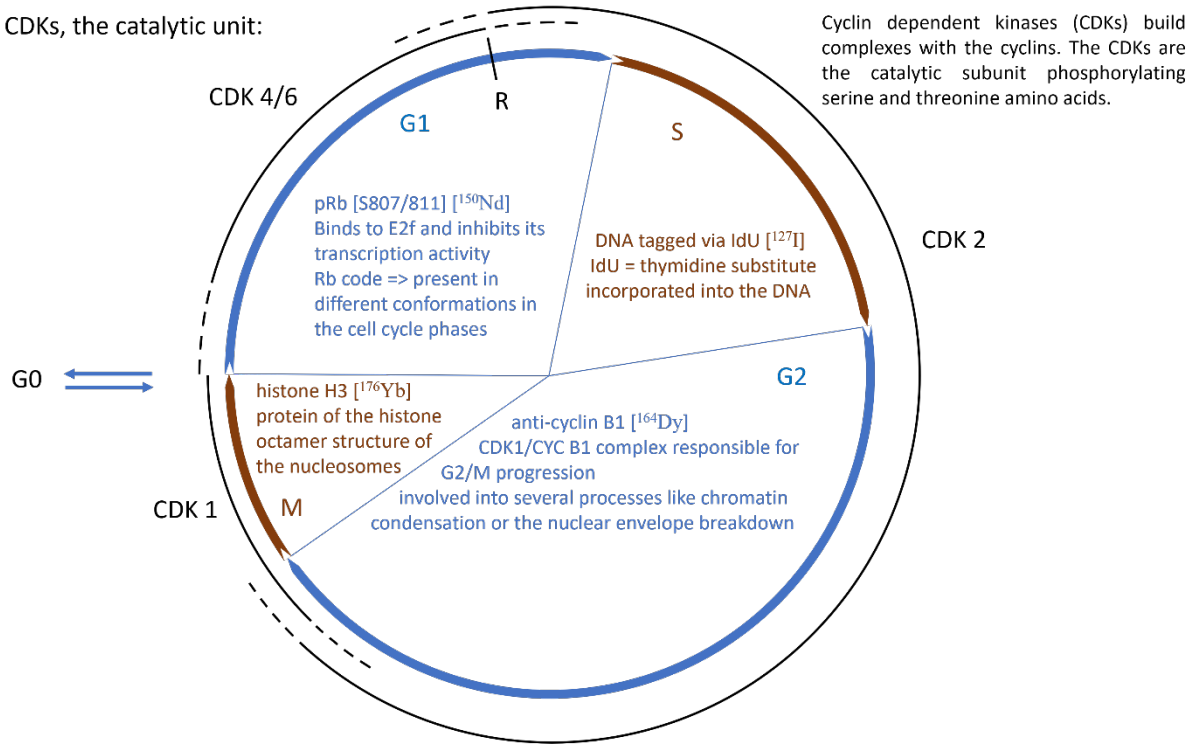

Scheme 1: Implication of the CDKs in cell cycle as well as the marker used for the tracking of the cell cycle phases.

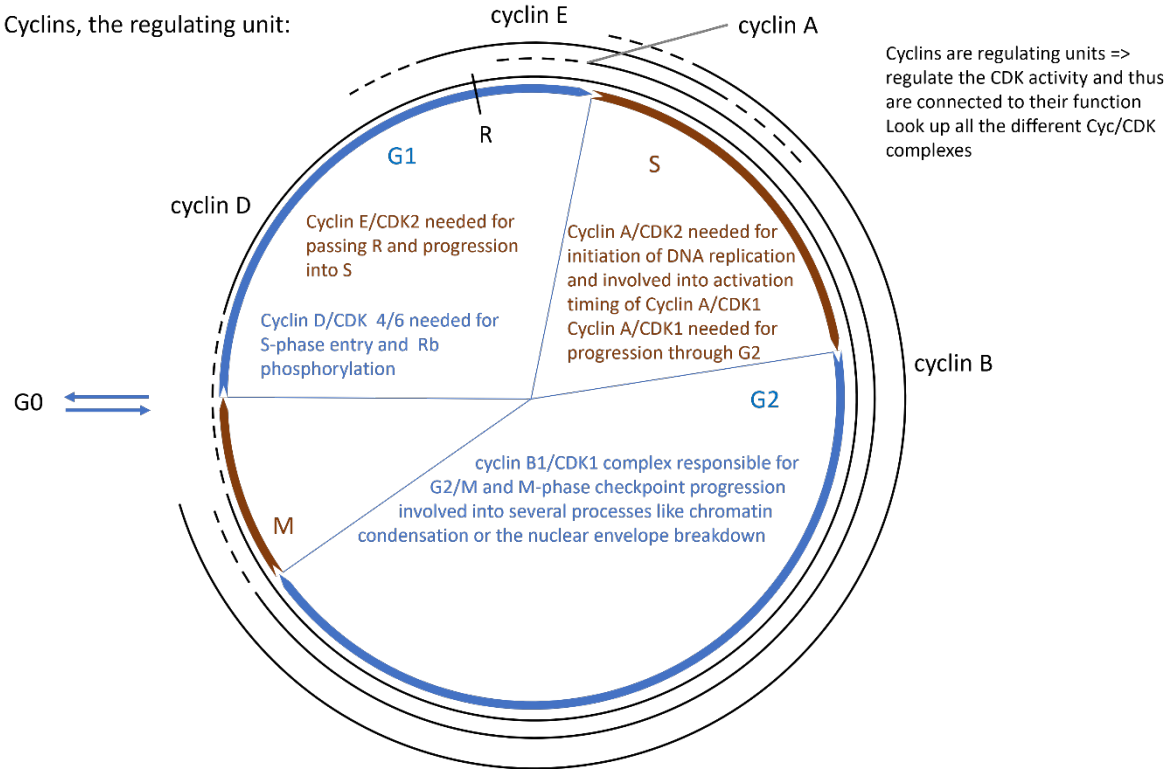

Scheme 2: Implication of the cyclin/CDK complexes in cell cycle, their function and the presence of the different cyclins in the cell cycle phases.

The G1-phase comprises the first so called checkpoint or restriction point within the cell cycle. This phase serves as a control to check if the cell contains enough nutrients and building blocks which are needed for the subsequent phase as well as cell organelles which are getting duplicated. Furthermore, it is getting checked if there is any DNA damage. For example in case of DNA-damage in form of DNA double-strand breaks, a p53-induced G1-cell cycle arrest is introduced.[12] Main actors for the progression through G1 are the cyclins D1, D2 and D3 and their catalytic partners CDK4 and CDK6. At the beginning of the cell cycle, these cyclins are expressed and bind to CDK4 and CDK6. This results in a phosphorylation and activation of the CDKs which can then carry out on of their enzymatic role, the phosphorylation of the retinoblastoma (Rb) protein [10, 13] However, for different organisms, the respective CDKs or Rb-proteins differ. So are inhibitors for the drosophila melanogaster the Rbf1 protein, for the saccharomyces cerevisiae (yeast) the Whi5 protein and for the homo sapiens the RB protein. So also differ the CDKs responsible for the phosphorylation of the respective inhibitors and co-repressors.[14] Within this work, the focus is lead to the human cell cycle and it´s mechanisms. The RB proteins are so called pocket proteins and come in different variations as for example the Rb/p105, p107 and Rb2/p139.[14-15] At the beginning of the G1-phase, RB-proteins are bound to transcription factors such as activator E2F proteins and thus inhibits them, whereas E2F4 proteins bind to Rb p130 and p107 at promoters to repress transcription.[14] Un- and hypophosphorylated RB binds E2F transcription proteins which is necessary for the transcription of several responder genes (e.g. cyclin E) needed to pass the restriction point R in late G1.When hyperphosphorylated, the Rb-protein is not decomposed until the end of the mitosis.[10, 16] The pRb protein might also have other functions within the cell during the cell cycle like for example the cell growth, apoptosis or how the cell interacts with the environment. This includes the interaction of cells with different cells or an extracellular matrix.[17] This is possible due to the pRb protein having 13 possible phosphorylation sites. Depending on which serine or threonine is phosphorylated, the structure changes and enables or disables the binding to a specific partner or protein such as the E2F. These different phosphorylation patterns and the respective change in function are often referred as the ‘pRb code’. Up to now, not all of the possible phosphorylation’s and the structural effects are known.[18] However it is known that the binding of un- and hypophosphorylated Rb to E2F isolates the E2F and inhibits its function. The pRb protein also represses gene transcription through the interaction with other proteins like hBRM, BRG1, HDAC1 or SUV39H1. With these interactions, the pRb-protein also influences the nucleosome remodeling, histone de-/acetylation, and methylation.[15] The pRb-protein thus influences gene transcription in more than one way. Whereas when further

phosphorylated by CDK4/6 to an hyperphosphorylated form, its affinity to E2F is reduced, E2F is split off and thus the inhibitory function of the retinoblastoma protein is lost. The E2F can finally fulfill its activity as an transcription protein.[10, 16] The loss of the pRb-protein function can thus plays an immense role in the dysregulation of the cell cycle homeostasis and lead to the development of retinoblastoms, malignant tumors on the retina.[15]

If at any moment of the G1 checkpoint a failure or inconsistency appears, the further progression into the S phases is interrupted. In case of DNA-damage, pre-existing p53 binds to a sequence-specific DNA site which leads to an induction of the synthesis of p53 itself.[10] This increase in p53 provokes a transcriptional upregulation of the CDK inhibitor (CKI) p21[19] which actively inhibits CDK2, 4 and 6. By inhibiting these CDKs, the phosphorylation of Rb is compromised which is needed for the progression from G1 to S.[10] Ghannam et al for example damaged the DNA of MDA-MB-231 breast cancer cells by exposing them to ASPE. The cells underwent a G1 cell cycle arrest showing upregulations of Cip/p21 and Kip1/p27, downregulations of cyclin D and cyclin E transcripts and their related CDKs, Cdk2, Cdk4 and Cdk6. However, in case of too much DNA-damage, the cells induced the apoptosis.[20] This gives the cell the time to repair the DNA damage. Whereas there are many more mechanisms and pathways involved into the cell cycle arrest within the G1-phase. Within this work, DNA damage is induced by incubating the cells with cisplatin which binds to the N7 of purine bases[21] within the DNA leading to 1,2-interstrand cross-links.[21-22] The induced DNA damage will consequently lead to a cell cycle arrest during phase G1 and S.[23] This mainly depends on the concentration of cisplatin used during the treatment of the cells. Lower concentration will lead mostly to an S-phase arrest whereas higher concentrations tend to an arrest within the G1-phase or to initiate apoptosis.[24] As previously stated, the G1-phase serves as checkpoint to check for DNA damages and if the cell has all the nutrients needed for the rest of the cell cycle as well as the starting of cell organelles being duplicated. When cells lack nutrients, they will undergo a cell cycle arrest in G1. However, the mechanism of the cell cycle arrest differs from the previous ones whereas here, the CDK2 activity is suppressed depending on Skp2 level whereas CDK4 activity is suppressed independently on the Skp2 level.[25]

For the overcoming of the G1-/S-phase transition, Cyclin E binds to CDK2 which enables the progression into the S-phase.[11] When successfully having passed the restriction point in the G1-phase, and progressed into the S-phase, the DNA is getting replicated so that all the genomic information can be passed to the two daughter cells during the mitosis. During the transition from G1- to the S-phase, Cyclin A is expressed and stays at high levels throughout the phase.

For the synthesis of the DNA itself, cyclin A must bind to CDK2 to activate its phosphorylation activities which is needed for the initiation of the DNA replication.[10] In the S-phase, it is important that the cells undergoes a single round of chromosomal DNA replication.[11] There is also a checkpoint in the S-phase to ensure a repair mechanism in case of DNA-damage or replication perturbations to maintain the genome integrity by stabilizing the replication fork.[26] After the successful replication of the DNA, the cell progresses from the S- into the G2-phase. This is enabled by the cyclin A/CDK2 complex. At the end of the S-phase, cyclin A will also bind to CDK1 to which leads the cell through the G2-phase. The cyclin A/CDK2 activity is also linked to the exit of the G2-phase for the transition into the M-phase by regulating the timing of the activation of the cyclin B1/CDK1 complex which is needed for the progression form the G2 into the M-phase.[27] The G2-phases is the second gap phase in which the DNA is getting checked for DNA-damage or wrong replication.[28] For the progression through the M-phase, the activity of the cyclin B-CDK1 complex is important as it influences the initiation of the protein synthesis whereas CDK1 has also other functions in the different cell cycle phases.[29] The cyclin B1-CDK1 complex is important for chromatin condensation[30] and the breakdown of the nuclear envelope. In the interphase, the cyclin B1 stays within the cytoplasm and is shuttled at beginning of the M-phase into the nucleus.[31] The miotic spindle checkpoint in the M-phase servers as control for the proper segregation of the sister chromatids. The spindle consists of several motor proteins as well as the microtubules. For the miotic checkpoint, it is important that the spindle microtubules are attached to both, the centrosomal and kinetochore ends and are under tension. The kinetochores also must be aligned for the progression through the M-phase. Furthermore, the DNA integrity is checked. The myotic cyclins are important for the inhibition of the CDKs activity which lead the process of the chromatid separation.[32] Taxol is highly affinitive to the tubulin protein and by binding to the tubulin protein, it promotes its dimerization and thus stabilizes the tubulin polymerization. This results in preventing the microtubules depolymerization which is needed for the progression though the mitosis and thus initiating an arrest in the M-phase.[25]

To be able to analyze different compositions of cell cycle phases, the cells are treated in four different ways to achieve different cell cycle arrests. The cell cultivation and treatment has been done by the Medical University of Vienna within the working group of Univ.-Prof. Dr. Berger. The treatments were done over a period of 24 hours. The first type of sample is the control sample (ctr). Nothing has been added during cell cultivation except medium and serum. Thus, the cell cycle distribution corresponds to the normal cell cycle distribution of the cell line. For the cisplatin treated sample (cis) there will be a cell cycle arrest in the phases G1 and S as

previously explained. The cisplatin treated samples were cultivated in a medium containing serum and a cisplatin concentration of 5 µM. For the taxol treated sample (tax), the cells have been cultivated in a medium containing serum and 30 nM of taxol. Taxol induces a cell cycle arrest in G2 and M-phase because it stabilizes tubulin polymerization which takes place in those two phases.[25] The last treatment is the 0% serum sample (ser) where the cells have been cultivated within a serum free medium. This should provoke a cell cycle arrest in G1.

One part of the works aim is to differentiate between the different cell cycle phases. This is achieved by tagging the phases in three different ways. One intercalator has been used, one DNA-building block which is directly getting incorporated into the DNA and several metal-labeled antibodies. The intercalator used is an iridium-based DNA-intercalator which enables the tracking of the DNA/nucleus within the cells. As all the cells contain DNA, this marker can be used for the visualization of all the cells and is also used as signal input for the segmentation.

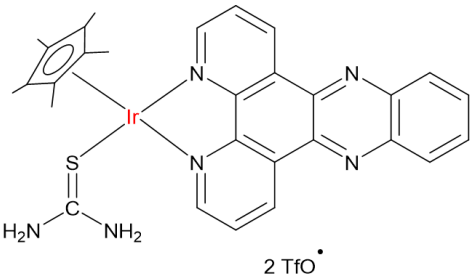

Scheme 4: Structure of the ^{193}Ir-intercalator.

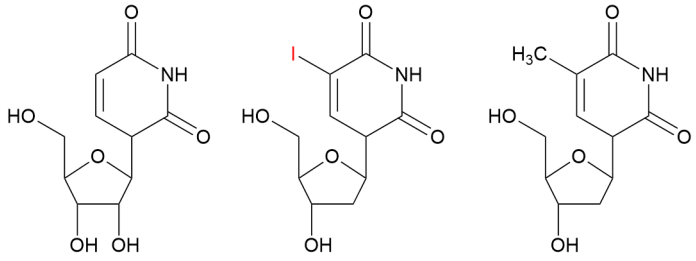

Scheme 3: Structure of uridine, ^{127}IdU and thymidine.

The building block which is getting incorporated into the DNA during the DNA synthesis is cell ID IdU (5-Iodo-2'-deoxyuridine) which is a uridine based analog and is recognized as thymidine substitute in DNA synthesis (Scheme 4). Thus, it gets incorporated into the DNA during the S-phase and represents a good marker if the cells in the S-phase do not pass into a subsequent phase. In this case, the cell would show the S-phase marker even though the cell is already in G2 or the M-phase.

The last types of markers are metal labeled antibodies which can specifically bind to proteins. The antibodies are conjugated with one isotope of a metal such as ^{150}Nd, ^{164}Dy, ^{168}Er or ^{176}Yb. These metals do not naturally occur within the cells and if a cell shows a signal for one of the markers, it must originate from the marker. The proteins tagged are the pRb-protein [S807/S811] (^{150}Nd), cyclin B1 (^{164}Dy), anti-KI67

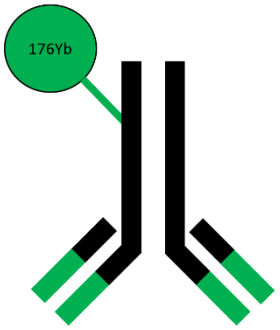

Scheme 5: Structure of a metal labeled antibody with ^{176}Yb as conjugated metal.

(^{168}Er) and histone H3 [S28] (HTA28) (^{176}Yb). The metals were added to the antibody by conjugating them to a polymer which can be bound to the antibody structure.

The function of the pRb and cyclin B1 have already partly been discussed previously. However, it must be kept in mind, that for all the proteins in the cell cycle, they are synthesized and degrade over time. Thus they can slightly be present in subsequent phases or for the pRb-protein, it is know that it might be present in different formations within the cell.[18] The KI67 is an proliferation marker protein which is within the nucleus during the G1, S and G2-phase and on the chromosomes during the M-phase.[33] However, it's expression is strongly downregulated within the G0 state. This makes it an optimal marker for the detection of proliferating cells and differentiate between the G0 state from the cell cycle phases.[33-34] KI-67 has several functions in the cell depending on the phase. Within the interphase KI-67 is needed for the normal cellular distribution of the heterochromatin antigens and for the nucleolar association of heterochromatin. During the mitosis however, KI-67 is required for the formation of the perichromosomal layer which prevents the aggregation of mitotic chromosomes. Whereas KI-67 has even more functions within the cell cycle phases.[35] The last marker is the histone H3 marker which is part of the histone octamer. One histone octamer consist out of pairs of four core histones, H2A, H2B, H3 and H4. The histone octamers when winding up the DNA will form the nucleosomes. Nucleosomes are the protein structure which have wind up the DNA during the M-phase to build the nucleosomes which form the chromosomes. So, the last marker is tagging histone H3 which is part of the protein structure responsible for the winding up of the DNA and backbone structure of the chromosomes. Whereas the synthesis of the histone is already initiated in the S-phase. When entering the M-phase, the histone H3 protein is phosphorylated. This phosphorylated version of the histone H3 protein is being tagged and is only found within the M-phase.[36]

It must be considered that the pRb-marker (G1) as well as the cyclin B1-marker (G2) are liquid markers which are typically used for liquid samples. The proliferation- and the histone H3-marker (M) however are tissue markers. Thus, for the G1-and G2-marker, there are no staining procedures available for cytospins.

When having successfully optimized the staining procedure for each marker, ideally a pipeline can be set up in order to simplify the workflow when it comes to the segmentation and the statistical evaluation. There are many different programs which could be used. However for this work, four segmentation programs have been used which were the most promising. HDIP, CellProfielr; Ilastik and cellpose. All showing their own advantages and disadvantages. The

setup of the pipelines has been done in cooperation with Gabriel Braun, PhD student at the University of Vienna within the working group of Univ.-Prof. Dr. Köllensperger. The statistical evaluation has been done based on R.

The cell cycle analysis based on CyTOF with the pRb-protein (G1), the IdU (S), the phosphorylated retinoblastoma protein [Ser807/811] (G1-phases), the anti-pS28HistoneH3 (M) and Ir-intercalator (nucleus) marker has already been done by Nolan et. al. Based on this review, the same cell cycle gating strategy has been used. The M-phase marker being very specific was the first phase to be assigned to the cells. The S-phase marker being very specific too was the second phase attributed. The G2- and G1-phase has been assigned as third, respectively as fourth phase. All cells left are cells within the G0-phase or are dead cells.[4] Stokke et al improved this method by using anti-CDT1 (G1), IdU (S), anti-Geminin (non-G1phases), anti-pS28HistoneH3 (M) and an Ir-intercalator (nucleus) to differentiate between the different cell cycle phases. However, they also differentiated between the early and late G1 and G2-phases by tagging the late G1-phase with an anti-pS780RB1 and the late G2 with an anti-PLK1 marker.[5]

Data for comparison has been acquired by fluorescence-activated cell sorting (FACS) which was executed by the Medical University of Vienna (working group of Univ.-Prof. Dr. Berger). The cells are treated with a fluorochrome which tags ribonucleic acids. Though the progression of the cell, the DNA duplicates. In the G1-phase, the DNA represents one equivalent of the total amount of DNA within a cell. During the S-phase, the DNA duplicates and the equivalent DNA within the cell is between 1 and 2. After the DNA has been duplicated in the S-phase, the cells contain 2 equivalents of DNA in the G2 and M-phase. For this reason, it can not be differentiated between the G2- and M-phase within the FACS measurement.

2. Aim of the work

Aim of this work is the development of an analytical method for the determination of the different cell cycle phases of different cell cultures in form of cytospins. For this, the cells are treated with different methods to arrest the cells in different cell cycle phases in order to analyze different compositions. The main method used for the visualization of the cell cycle phases is laser ablation in combination with inductively coupled plasma time-of-flight mass spectrometry (LA-ICP-TOFMS). Beforehand, an adequate sample preparation must be set up and optimized for the staining with metal labeled antibodies and markers in order to be able to visualize the fours cell cycle phases as well as the DNA. In cooperation with a bioinformation, four segmentation methods have been tested and pipelines have been set up for the optimal segmentation of the cytospins. This data and method enable a fast and easy statistical evaluation of a defined cell population according to their cell cycle phase that they are in with R. The method will serve for screening cellular metal based candidate drugs accumulation with regard to cell cycle.

3. Experimental

3.1 Chemicals and reagents

The laboratory work including sample preparation and staining was performed in the laboratory 1, room 1234 in Währinger Straße 38; 1090 Vienna, Austria. The preparation of the antibody cocktails and final washing steps with ultrapure water were performed in a cleanroom ISO-class 8 (FED STD 209Eequivalent class 100000) (room 1240A, Währinger Straße 38; 1090 Vienna, Austria). The measurements via LA-ICP-TOFMS were performed in a cleanroom ISO-class 7 (FED STD 209Eequivalent class 100000) (room 1240A, Währinger Straße 38; 1090 Vienna, Austria).

Ultrapure water (18.2 MΩ cm, ELGA Water purification system, purelab Ultra MK 2, UK) was used for the staining, dilution and washing steps of the markers. The four metal-based antibodies (Anti-KI-67, Anti-pHistone H3 [Ser28], Anti-pRb [S807/S811] and Anti-cyclin B1), the Cell-ID™ IdU and the Cell-ID™ Intercalator-Ir (Cell-IDTM, 125 µM) were purchased from Fluidigm (now Standard BioTools, San Francisco, CA). Tween™ 20 Surfact-Amps™ Detergent was purchased from Thermo Scientific. Triton™ X-100 (for molecular biology) and Tris buffered saline (TBS) (BioUltra) were purchased from Sigma Aldrich (Steinheim, Germany). The Dako target retrieval solution (pH 9) for antigen retrieval was purchased from Agilent Technologies (Waldbronn, Germany). Taxol was purchased from Bristol-Meyers Squibb (Latina, Italien)

All cell culture media and reagents were purchased from Sigma-Aldrich (St. Louis, MO) and unless stated otherwise, all plastic dishes, flasks, and plates were obtained from StarLab (Hamburg, Germany). Cisplatin was synthesized at the Institute of Inorganic Chemistry, University of Vienna, according to literature procedures.[37] TrypLE Express with phenol red (Gibco, Fisher Scientific, Roskilde, Denmark) and Typsin (Gibco, Fisher Scientific, Roskilde, Denmark) was used for the cell detachment from culture plastic according to the manufacturer instructions. Prodinium Iodide (PI; 1 mg/ml; P4864) was obtained from Sigma-Aldrich. The FACS-PBS contains RNAse (Ribolock RNAse Inhibitor, E00381) inhibitor from Thermo Fisher Scientific.

3.2 Sample material, cell culture and treatment

The human A2780 ovarian cancer cell line, obtained from Sigma-Aldrich and the aneuploid immortal keratinocyte HaCaT cell line from adult human skin from the center of cancer research (Prof. Dr. Eibling) were seeded in 6-well plates (for cell suspension, FACS measurements and cytospins) and maintained in Roswell Park Memorial Institute (RPMI) 1640 (Sigma-Aldrich) culture medium supplemented with 10% fetal calf serum (biowest, VWR) at 37 °C and 5 % CO_2 in a humidfied tissue culture incubator. The cell cultures were treated with different compounds (serum free medium, 30 nM Taxol or 5 µM Cisplatin) over a period of 24 hours followed by an incubation with Cell ID IdU for 30 or 60 minutes.

To prepare the cytospins, the cells were detached using TrypLE™ Express or Trypsin and were subsequently washed twice with TBS. The cytospins were prepared using with a Cytospin 4 Centrifuge (Thermo Scientific) at 350 rpm for 5 minutes. The glass slides were dried at RT for 30 minutes, fixed with 4% PFA for 20 minutes and washed twice with water. The cytospins were finally dried at room temperature.

3.3 Data Processing

The LA-ICP-TOFMS raw data were further processed in HDIP-v1.7.4.22ed5789, a laser ablation software provided by Teledyne Photon Machines (Bozeman, MT). Also, the raw TIFF-files were exported via HDIP without any manipulation of the data.

CellProfiler-v4.2.1 was used for segmentation as well as for the data processing of other segmentation methods. Ilastik-v1.3.3post3 was used as segmentation method. Miniconda-v4.12.0 was used to run cellpose-v1.0[38] and -v2.0[39] based on the nucleus model which was also used for segmentation. R was exclusively used on version 4.1.2 for the data processing, the statistical analysis and the creation of the figures used in this work. The FACS analysis has been done with FlowJo-v10.06 (BD Biosciences).

3.4 FACS measurements

The A2780 and HaCaT cells were each plated into 6-well plates (1×10^6 cells/well per cell line) and allowed to adhere over a period of 24 h. Each well has been incubated for another period of 24 h with either serum free medium, medium containing 5µM cisplatin or 30 nM taxol. Also, one control sample has been cultivated without any treatment. Cell cycle progression was

analyzed by collecting the cells, washing them with PBS, recovering them in a 0.9% NaCl solution (100 µL), transferring them drop by drop into ice-cold alcohol (70%; 1.8 ml) and storing them at -20°C overnight. When analyzed, each sample was centrifugated at 8000 rpm for 2 minutes and incubated for 30 min at 37°C with FACS-PBS containing RNAse (10 µg/mL). After a treatment with 5 µl of prodinium iodide for 30 min at 4°C, the FACS measurement was done with an LSRFortessa flow cytometer (BD Biosciences, NJ, USA). The software FlowJo-v10.06 (BioSciences, NJ, USA) was used to analyze the resulting DNA histograms.

3.5 Staining parameters for the different samples and LA-ICP-TOFMS measurement

For the staining of the samples, two different blocking solutions and permeabilization methods have been used. The TBS used were prepared by dissolving two pellets of TBS in ultrapure water (1 L).

3.5.1 Staining of A2780 cells

As a first step, antigen retrieval was performed by incubating the cytospins in a Dako target pH 9 retrieval solution at 96 °C for 30 min. The samples were washed using ultrapure water for 10 minutes and permeabilized by incubation with Triton^{TM} X-100 twice for 8 min. The samples were washed again in ultrapure water for 10 minutes and in TBS for another 10 minutes. Next, blocking of unspecific binding sites was performed by incubating the cytospins with 3% BSA in TBS for 45 min in a hydration chamber. The cytospins were then incubated with an anti-cyclin B1, anti-pRb-protein, anti-Histone H3 and an anti-Ki67 (all 1:100 diluted in 0.5% BSA in TBS) antibody cocktail over night at 4 °C in a hydration chamber. The next day, the cytospins were washed three consecutive times with TBS. The staining of the nuclei was performed by incubating the cytospins with an Ir-intercalator (1:400 dilution) for 30 min at 4 °C in a hydration chamber. After nuclei staining, the cytospins were washed twice with ultrapure water for 10 minutes each and air dried at room temperature.

3.5.2 Staining of HaCaT

As a first step, antigen retrieval was performed by incubating the cytospins in a Dako target pH 9 retrieval solution at 96 °C for 30 min. The cytospins were washed using ultrapure water for 10 minutes and permeabilized by incubation with 0.05% Tween and TBS. The cytospins were

air dried and blocking of unspecific binding sites was performed by incubating the cyctospins with a 3% BSA-TBS solution for 30 minutes in a hydration chamber. The blocking solution was removed and a mixture of CD16/CD32:TBS (2:198 µl) has been added to each sample for 10 minutes. Antibody staining was performed differently depending on the sample. The compositions of the antibody cocktails are listed in Table 1. The prepared antibody cocktails were centrifugated at 13000 ref for 2 minutes. The staining was performed over night at 4°C with the respective antibody cocktail. The main samples are the samples used for the analysis (part 4.3.9) whereas the two optimization attempts were used for part 4.3.6 to improve the G1- and G2-marker.

Table 1: List of the composition of the antibody cocktails used for the four main HaCaT samples which has been used for the evaluation as well as for the first try of the optimization of the G1 and G2 marker (Opti 1) which corresponds to a dilution series.

	main samples	diluted series (Opti 1)
10% BSA	10 µl	5 µl
M marker	2 µl	1 µl
Proliferation marker	4 µl	0.5 µl
G1 marker	4 µl	0.5 µl
G2 marker	4 µl	0.5 µl
CD16/CD32	2 µl	1 µl
TBS/TWEEN 0.05%	174 µl	91.5 µl
total volume:	200 µl	100 µl

For the second optimization attempt the sample was stained twice. Antibody staining for the M-phase was performed overnight (Table 2; Antibody cocktail 1 (opti 2) at 4°C in a hydration chamber. Antibody staining for the G1 and G2-phase as well as the proliferation marker was performed (Table 2; Antibody cocktail 2 (opti 2) at room temperature for 30 min in an hydration chamber.

Table 2: List of the composition of the antibody cocktails used for the second optimization attempt of the G1 and G2 marker. The antibody cocktail number 1 is for the staining of the M phase at 4°C over night and the second antibody cocktail for the staining of the G1, G2 and proliferation marker at RT for 30 minutes with a dilution of 1:100.

	Antibody cocktail 1 (opti 2)	Antibody cocktail 2 (opti 2)
10% BSA	2.5 µl	2.5 µl
M marker	0.5 µl	/
Proliferation marker	/	0.5 µl
G1 marker	/	0.5 µl
G2 marker	/	0.5 µl
CD16/CD32	0.5 µl	0.5 µl
TBS/TWEEN 0.05%	46.5 µl	45.5 µl
total volume:	50 µl	50 µl

After the antibody staining, the cytospins have been washed three times with TBS/TWEEN 0.05% for 5 minutes each. The next day, the cytospins were washed three consecutive times with TBS/TWEEN 0.05%. The staining of the nuclei was performed by incubating the cytospins with an Ir-intercalator (1:100 dilution) for 5 min at 4 °C in a hydration chamber. After nuclei staining, the cytospins were washed twice with ultrapure water for 5 minutes and air dried at room temperature.

3.6 LA-ICP-TOFMS

For the LA-ICP-TOFMS measurements, an Iridia 193 nm laser ablation system from Teledyne Photon Machines (Bozeman, MT), equipped with an ultrafast low dispersion cell[40] in a cobalt ablation chamber, was coupled with an icpTOF 2R ICP-TOFMS instrument from TOFWERK AG (Thun, Switzerland). An aerosol rapid introduction system (ARIS) was used which mixed an Ar makeup gas flow (with a flow rate of 0.90 $\frac{\mathrm{L}}{\mathrm{min}^{-1}}$) with an optimized He carrier gas flow (with a flow rate of 0.60 $\frac{\mathrm{L}}{\mathrm{min}^{-1}}$) before entering the plasma of the ICP-MS. Laser ablation and ICP-TOFMS settings were optimized daily. For this optimization, a maximum sensitivity for the elements $^{26}Mg^{+}$, $^{59}Co^{+}$, $^{115}In^{+}$, and $^{238}U^{+}$ was attained. Laser-induced elemental fractionation was reduced based on the $^{238}U^{+}/^{232}Th^{+}$ ratio (±1) and oxidative levels based on the optimization of the $^{238}U^{16}O^{+}/^{238}U^{+}$ ratio (< 2%). For these optimization measurements, a NIST SRM612 glass-certified reference material from the National Institute for Standards and Technology (Gaithersburg, MD) has been used. Laser ablation was exclusively performed using a circular spot size of 1 - 4 µm depending on the sample. A fixed dosage of 2 has been used, line scans were overlapping by half in the y-direction resulting in pixel sizes of 0.5 × 0.5 to 2 × 2 µm^2. A repetition rate of 200-250 Hz and a fluence of 1.0 – 1.5 J cm^{-2} were used. The integration and read-out rate were optimized to match the laser ablation repetition rate. The integration as well as the read-out rate were optimized in a way to match the laser ablation repetition rate. Aim was to achieve a complete ablation of the cytospins without ablating the glass slides. The used fluence can differ for the same spot size depending on the sample.

Two different operation modes have been used. For the A2780 cytospins, a standard operation mode and for the HaCaT cytospins, a collision mode (CCT) was used which balance sensitivity, mass resolving power and ion transmission across the measured mass range which allows the analysis of all the ions with a mass to charge ratio from 14 to 256.

4 Results and Discussion

The result and discussion section will be split into three parts including the development of the method, the staining with its challenges as well as the validation and its challenges.

4.1 Setting up the method

Within this part of the discussion, the problems which have occurred during the method development are going to be explained. Here optimization can take place on different levels like the cell cultivation, the staining process of IdU, the making of the cytospins, the measurement parameters and the processing of the data.

4.1.1 Optimization of the laser parameters:

In a first step, the optimal measurement parameters had to be determined. For this, several laser spot sizes with different fluences have been tested (Table 3). The optimal conditions have been selected by different criteria like the intensities of the different marker signals and the final usability of the image. Too small spot sizes lead to lower signal intensities (CPS) which becomes problematic if the LOD is surpassed. Thus, the signal can not be used for the determination of the cell cycle phases. Furthermore, segmentation gets harder, the smaller the intensities are as the background signal gets closer to the actual signal of the markers. This blurs the boundaries between the background and the cell boundaries which leads to a wrong segmentation. Whereas too large spot sizes are counterproductive for the segmentation of the cells too. The segmentation of the cells is achieved by the visual detection of the ^{193}Ir- and ^{63}Cu-signal boundaries of the DNA and cells. To large spot sizes, so an insufficient resolution, leads to the possibility, that parts of cells are ablated within one laser shot. Hence, the boundaries between cells vanish and no proper segmentation can be done. This restricts the identification of single cells which is one of the main goals of this master thesis. The optimal parameters for the A2780 cell line have been an overlapping spot size of 2 µm, a fluence of 1.3 J/cm^2, a repetition rate of 200 – 250 depending on the daily tune of the MS settings, a dosage of 1 and at fixed dosage. The ^{193}Ir-signals captured for the four ablated samples with different spot sizes are illustrated in Figure 1. For the HaCaT cytospins, an overlapping spot size of 2 µm with a fluence of 1.5 J/cm^2 has been used due to an optimized staining procedure a better resolution for segmentation. A smaller spot size also leads to longer measurement time.

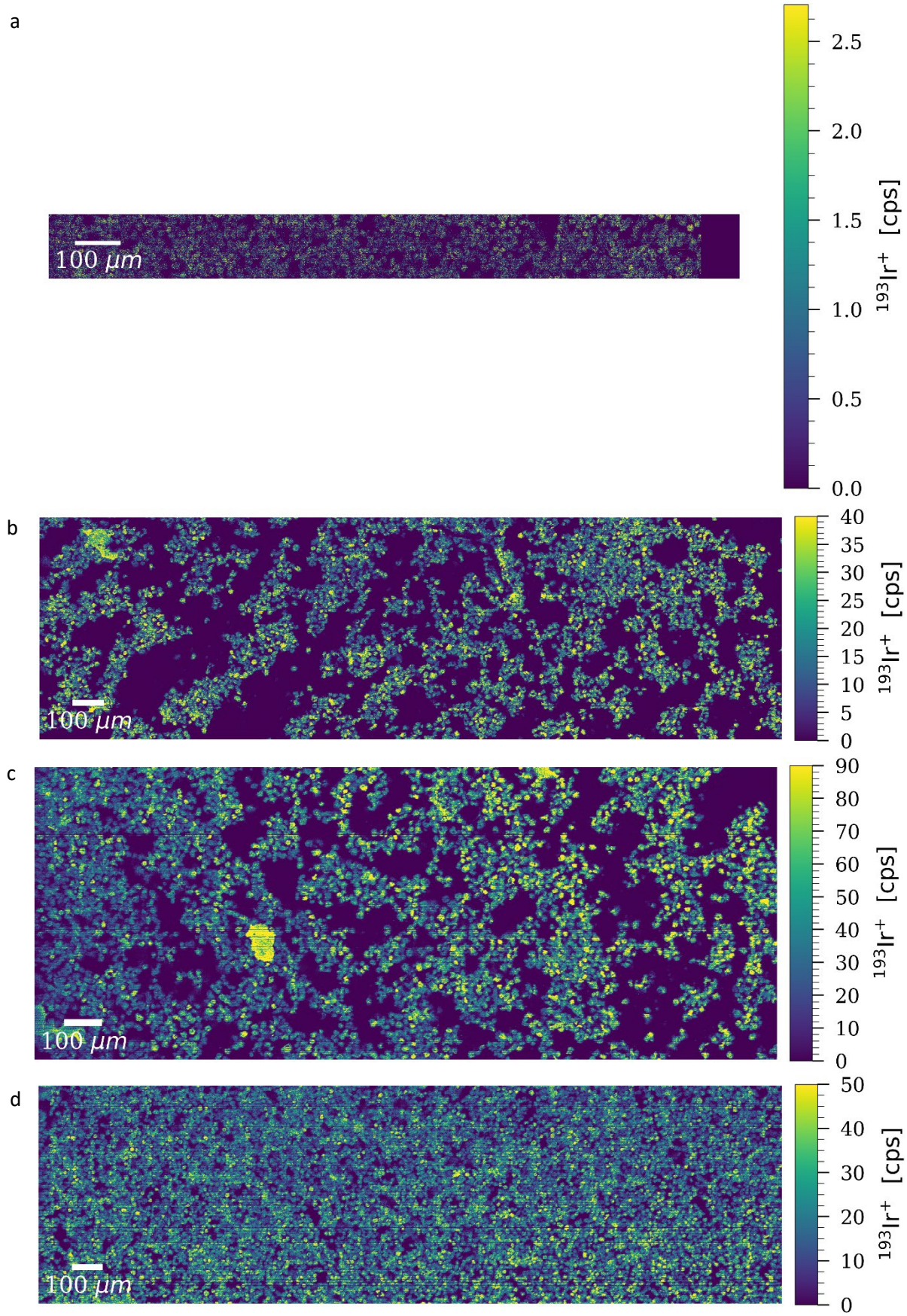

Figure 1: LA-ICP-TOFMS images of the ^{193}Ir-signal A2780 taxol treated samples used for the optimization of the LA-settings. Used final spot sizes and fluences are listed in Table 3.

Table 3: Optimization parameters of the laser for the analysis of the A2780 cell lines via LA-ICP-TOFMS.

final spot size [um]	fluence [$\frac{J}{cm^2}$]	Figure 1
0.5	1.5	a
1	1.3	b
1.5	1.1	c
2	1.0	d

4.1.2 Optimization of the cell cultivation and the making of the cytospins

The optimization of the cell cultivation and the making of the cytospins has been done by the Medical University of Vienna. The only process which has been changed depending on the cell line and treatment are the trypsinization which has mainly been done with trypsin whereas for some samples it was replaced with TripLE because of its effectiveness and as it is not as harsh for the cells compared to trypsin. This was done because for some cultures, the detachment of the cells from the flask did not work with trypsin. For the formation of the cytospins, different cell concentrations have been tested whereas no overall best cell concentration could be determined. The reason for this is because for the same cell concentration, the cytospins look very differently. So, for the same setup with the same cell concentration and the same cell culture and treatment, differently shaped and dense cytospins were obtained. The density of the cells on the cytospins even differed on the same cytospin (Figure 2). Optimal dense cytospins for this work would be cytospins with maximum density without cells touching each other. This facilitates and accelerates the segmentation as mismatches are less likely to occur which have to be corrected manually.

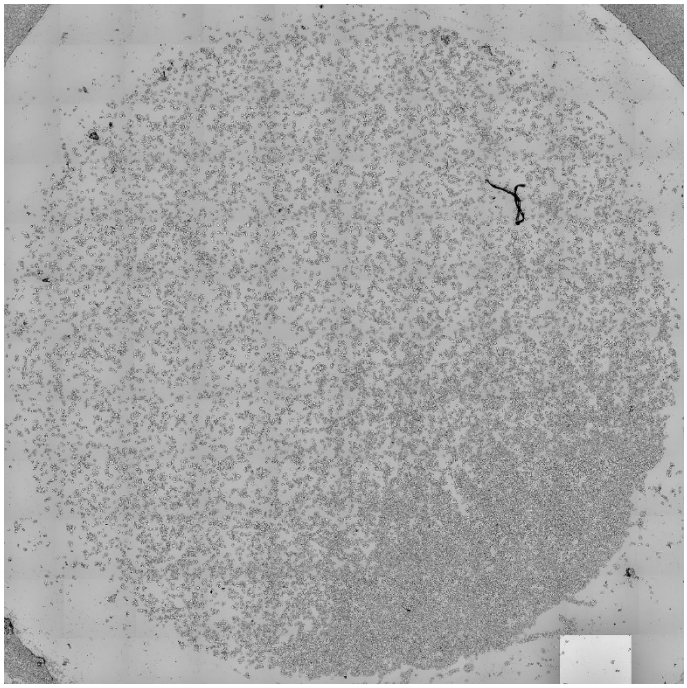

Figure 2: Cytospin of the HaCaT control sample showing different cell densities on the same cytospin.

Cells which have been treated with taxol undergo more likely a cell cycle arrest in the G2- and M-phase. During the cell cycle progression from G1- to the M-phase, the cells growth. In general, cells in the G1-phase should thus show the smallest mean area, followed by the S-phase and the cells in the G2- and M-phase have the biggest area per cell. Cell volume growth is close

to exponentially and cells grow at a higher rate in S-G2 compared to the G1-phase. However cell growth heavily depends on the cell line and even for a precise cell line (e.g. HeLa cells, cervical cancer cells), a newborn cell growth much faster compared to older cells in G1. Furthermore, for HeLa-cells, cell growth is linked to the cell size and thus contributes to the cell cycle homeostasis. [41] This increase in volume growth could indirectly be reinforced by the measurements of the area of the cells which has been evaluated for every sample (part 4.3.9). The taxol treated sample should for his reason have the highest mean area per cell as the cells are the biggest in the M-phase. The 0% serum sample should ultimately have the smallest mean area per cell as most of the cell will be arrested in the G1-phase. The cisplatin treated cells should undergo partly a G1 cell cycle arrest but mainly an S-phase arrest and thus, the mean area of all the cells should be in between the taxol treated sample and the 0% serum sample. This is also one reason, that for the different treatments, different cell concentrations have to be used and no overall cell concentration can be determined. The control sample having no precise cell cycle arrest but rather the normal distribution of the cell cycle phases, the respective mean area per cell can hardly be predicted. Whereas the M- and G2-phase lasting the shortest and the G1- and S-phase the longest, more cells should be in the G1- and S-phase for rapidly proliferating human cells.[10] Whereas this also depends on the cell line and no explicit data was found for the HaCaT cell line. The mean area per cell for the control sample is thus expected to be approximately in the magnitude of the cisplatin and 0% serum sample. The mean area per cell for the four treatments of the HaCaT sample are listed in Table 4. The taxol treated sample shows 25% bigger cells than the 0% serum sample and 18% bigger cells than the cisplatin treated sample. The cells in the control sample are slightly bigger (3%) than the cells from the cisplatin treated sample. The above stated theoretical part thus fits the measured data.

Table 4: listing of the cells detected, the theoretical cell cycle arrest for each treatment as well as the mean area per cell for the four treatments of the HaCaT sample.

Taxol:	Cells detected	Theoretical cell cycle arrest	Mean number of pixels per cell
Taxol	1175	G2/M	539
Cisplatin	1034	S	441
0% Serum	1144	G1	405
Control	1046	/[1]	455

[1]The distribution of the control sample corresponds to the natural cell cycle phase distribution and no special cell cycle arrest was aimed.

4.1.3 Segmentation problems concerning the sample

The first cytospins received (A2780 cell culture) were too dense for a proper segmentation via HDIP and CellProfiler, the two only used segmentation programs at that time. The optimal segmentation parameters differ for each sample and no overall parameters can be used. This results in mismatches during the cell segmentation, where the algorithm recognizes two or more cells near each other as one cell. These mismatches are more probable, the denser the cytospins are, especially when cells are touching each other. That is why when looking from a segmentation and statistical evaluation standpoint, optimal cytospins would be the densest sample possible without cells touching each other. This enables a proper segmentation with the highest data input possible. Whereas some cells are not segmented at all, especially for the segmentation with HDIP and CellProfiler. The reason for this can not be explained and when broadening the segmentation parameters, there are more additional mismatches compared to additional segmented single cells. The problem was simplified by making new, less dense cytospins. The difference in density of the A2780 and HaCaT cytospins is illustrated in Figure 3. Instead of using the A2780 human ovarian cancer cell line, a new HaCaT cell line has been used. The change in cell culture is due to a different uncertainty (part 4.3.5) The difference between the different segmentation methods will be discussed in part 4.1.6.

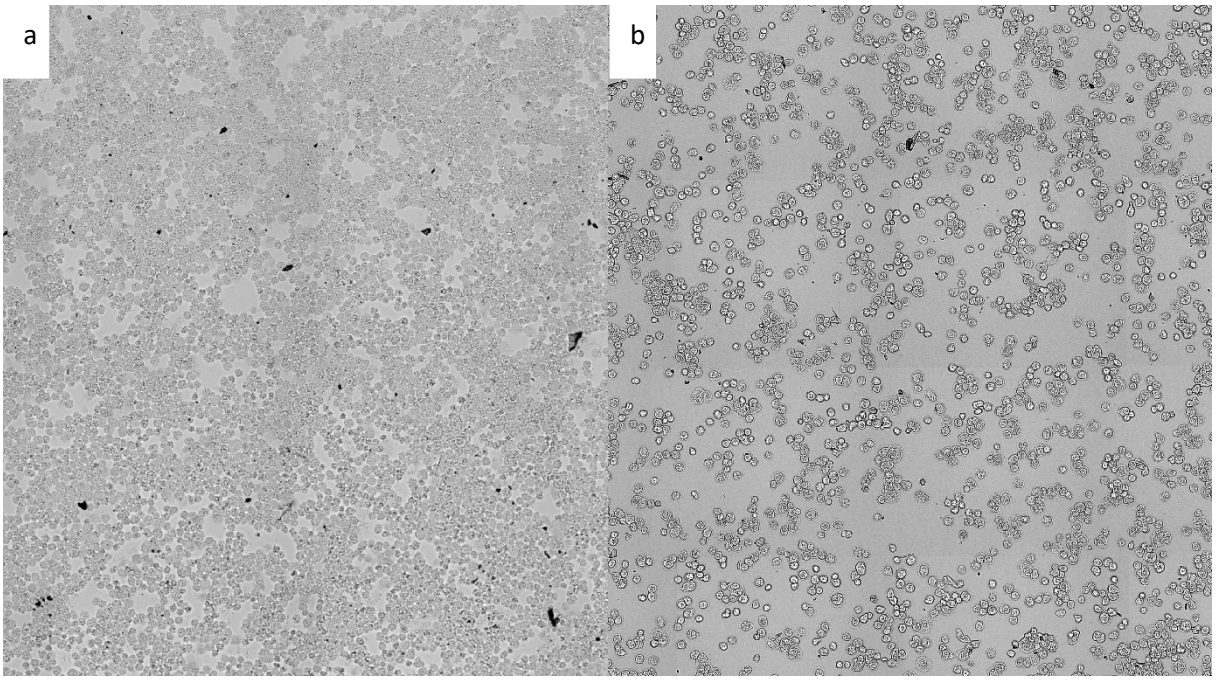

Figure 3: Comparison of two differently dense cytospins. a: first A2780 cytospin; b: new HaCaT cytospins.

4.1.4 High background signal of ^{127}I

The S-phase signal originally originating from the cell ID-IdU shows a very high overall background signal not only within the cells, but rather all over the ablated area. This complicates thresholding as there is no real or just a small separation between cells in the S-phase and cells in a different phase. The glass slides have a coating which facilitates the clinging of the cells on the surface of the glass. This coating is uniformly spread over the glass slide and would explain the uniformly higher ^{127}I-background. This could easily be avoided by replacing the coated glass slides with non-coated glass slides. When ablating such a non-coated glass slide, the ^{127}I-background intensity did not change. Thus, the coating was not the origin of the problem. More problematic would be to remove the ^{127}I-background if it originates from the laser- or argon-gas. When measuring the ion background while no sample is ablated, an ^{127}I-background is still detected. This leads to the assumption that the laser- or argon-plasma contains an ^{127}I-based impurity. This could be solved by purifying the gas or buying a different, non-contaminated gas. The uniformly high ^{127}I-background can be seen in Figure 4a showing a taxol treated A2780 sample and Figure 4b an taxol treated HaCaT sample. This figure also shows the distribution of the ^{193}Ir-signal and thus the cells to compare the cell distribution to the high ^{127}I-background signal.

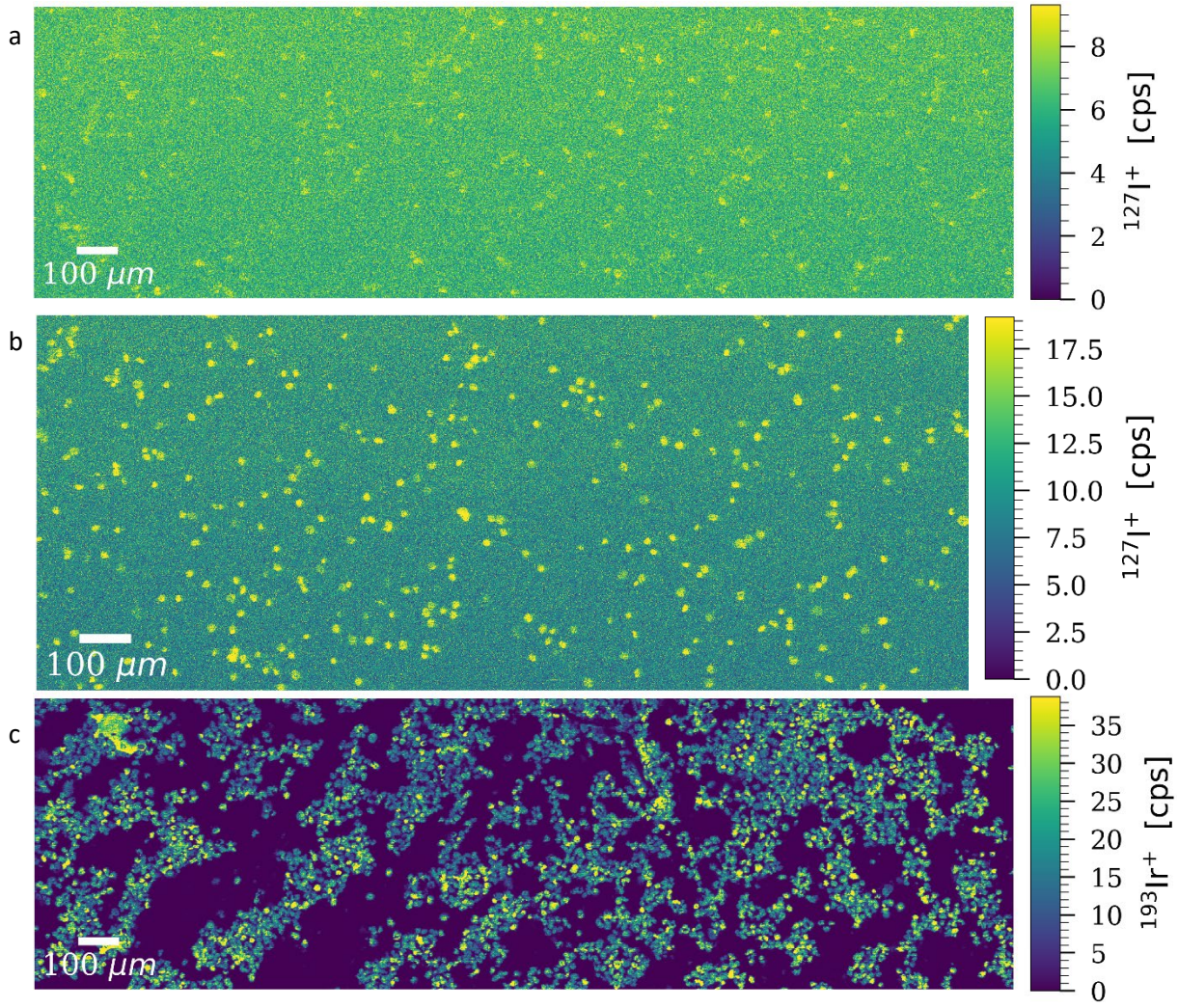

Figure 4: (a) Raw data of the taxol treated A2780 sample showing the ^{127}I distribution and the overall high background intensities (b) Raw data of the taxol treated HaCaT sample showing the ^{127}I distribution and the overall high background intensities but higher signals originating from the cells compared to a. (c) Raw data of the ^{193}Ir distribution for the comparison between the background of the ^{127}I signal and the non-contaminated ^{193}Ir-marker signal.

An indirect and easier solution for this problem would be by incubating the cells longer with IdU (60 min instead of 30 min) in order to elevate the signal originating from the cells from the ^{127}I-background. Basically, the contamination is not removed but higher signals from the cells leads to a separation between the signal from cells in the S-phase and iodine from the gas. Here it needs to be checked, if the cells are already passing from the S-Phase into one a subsequent phase because of the longer incubation with IdU. This would lead to incorrect assignments especially for the G2-phase because the G2-phase is attributed after the S-phase. In Figure 5 are the raw images of two control samples for the A2780 cell line (Figure 5a) and for the HaCaT cell line (Figure 5b). The ^{127}I-signal intensity for the 30 minutes incubation has a general intensity of 15 cps whereas for the 60 minutes incubation with IdU a general intensity of 21 cps

for positive cells. Thus the longer incubation with cell ID IdU led to an increase in the signal intensity. Thus the longer incubation with cell ID IdU led to an increase in the signal intensity.

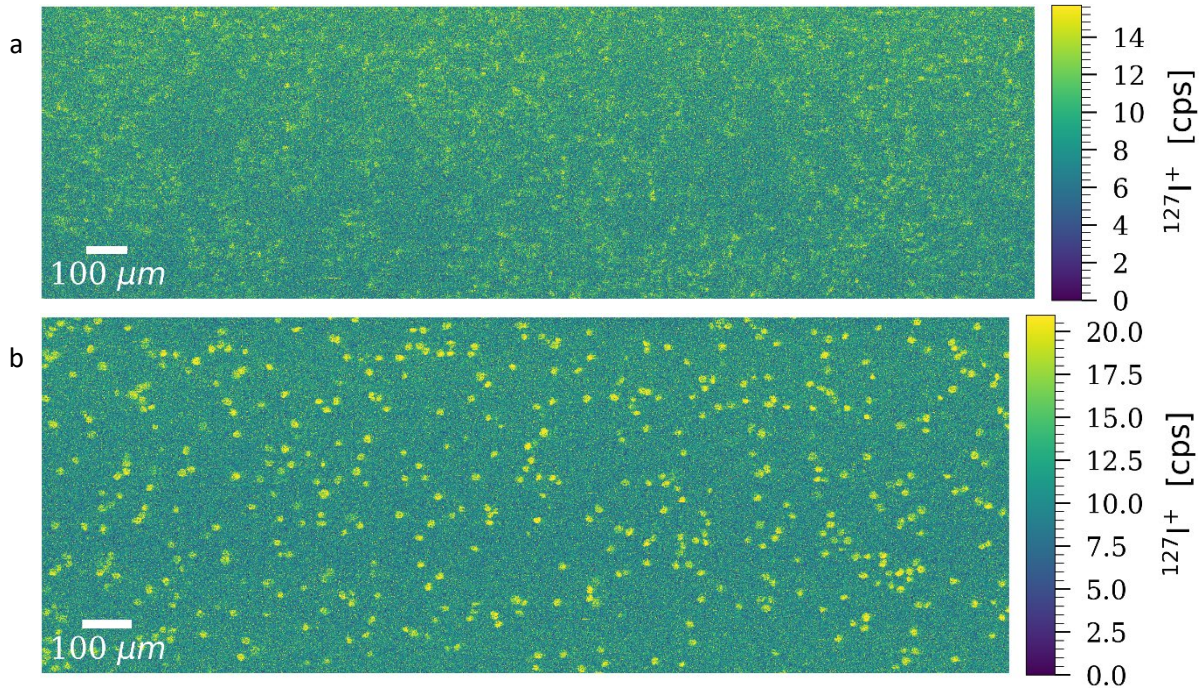

Figure 5: Raw data from two control samples showing the ^{127}I signal and an overall high background signal whereas cells can clearly be identified in the HaCaT sample (b) compared to the A2780 sample (a). the maximum intensity is higher in the HaCaT sample.

In Figure 6a are the overlap of the S-phase marker and the G2- or M-phase markers illustrated for an HaCaT control sample with 60 minutes of incubation time for the IdU. The HaCaT samples have been measured with the use of a collision gas compared to the s2780 samples which have not been measured in the CCT-mode. All cells being in the S-phase also show the G2-phase marker. The reason for this however does not come from the longer incubation with the IdU but rather due to the unspecificity of the G2-marker. More details to this will be presented in part 4.3.5.

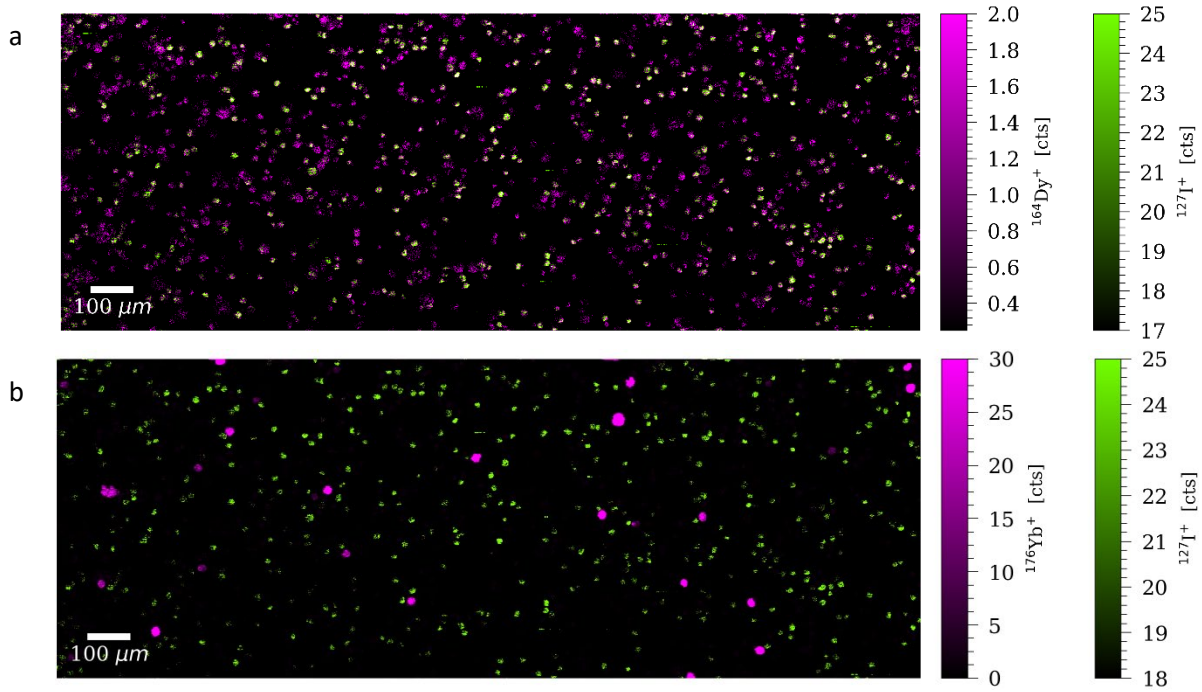

Figure 6: Overlay of the ^{127}I signal and the ^{164}Dy- (a) or ^{176}Yb signal from an HaCaT control sample which has been incubated for 60 minutes with IdU.

According to the FACS data. the cisplatin sample shows no cells within the G2-phase. However, when looking at the raw image, it is obvious, that cells have incorporated the G2 marker. This reinforces the hypothesis of the G2-marker being unspecific. See part 4.3.4. Cells already progressed from the S phase into the M phase would not be an obstacle as the M-phase is assigned before the S-phase. There are also no cells which show simultaneously a signal for the S- and the M-phase makers (Figure 6b). So, no cells have already progressed from the S-phase into the M-phase. To conclude, the optimization of the IdU staining parameters for the tracking of the S-phase was successful as it is now possible to assign the S-phase. At the time of this decision to incubate the cells longer with IdU during the cell cultivation, there was no good segmentation method available and the only samples available were the too dense A2780 cytospins. The decision was thus based on the visual evaluation of the raw data as well as a poor segmentation.

It must be considered that different cell lines have been used. The usage of different permeabilization methods during the saining of the markers should not have any influence as the staining with IdU is done during the cell cultivation. The A2780 cell line has been treated with Triton^{TM} X-100 whereas the HaCaT cells have been permeabilized with Tween (see part 3.5.2). The different cell line used might however have an impact on the uptake and incorporation of the IdU. Not only the fact that different cell lines have been used but also that the different cell lines are once a cancer cell line and once a healthy immortalized cell line

which might also have an impact on the uptake and incorporation of the IdU as cancer and healthy cells have a different cell cycle homeostasis. The cell cycle homeostasis of cancer cells is dysregulated, and the DNA content can differ in cancer cell lines (hyperploidy).[42]

4.1.5 Segmentation based on endogenous elements, impurities, or the DNA-marker

The segmentation itself can be done based on several signals. One possibility would be to use endogenous elements as ^{31}P as it has already previously been used as cell visualization method in tissue samples and can be used to compensate for the thickness of tissue samples.[43] As every cell contains phosphorous, it could be used as data input for segmentation. For the HaCaT samples however, a collision gas consisting of He and H_2 has been used in order to increase the sensitivity of higher mass elements, as most metals from the markers have higher masses which improves the usability of the raw data received. Due to the usage of this collision gas, the sensitivity of the elements with lower masses such as ^{31}P, is decreased. However, with further tweaks and changes, this could be optimized in further measurements. For this reason, the endogenous, low in mass elements can not be used for the segmentation for these measurements. In this work, ^{63}Cu and ^{193}Ir are used for segmentation. The ^{193}Ir-signal coming from the DNA-intercalator is only tagging the DNA and does not show the complete dimension of the cell. So, the histone marker and the S-phase marker (IdU) show a nearly complete overlap with the ^{193}Ir-signal as they mark the structure that winds up the DNA (histones) or get directly incorporated into the DNA (IdU). The overlaps of the M- and S-phase markers with the ^{193}Ir-signal are illustrated in Appendix 2a-b. Whereas the pRb (G1) and cyclin B1 marker (G2) are present in the whole cell and not only near the DNA and thus do not show a perfect overlap with the ^{193}I-rsignal but rather with the ^{63}Cu-signal (Appendix 2 c-d). ^{63}Cu is a contamination originating from the staining process and is present in all of the cell, not only near the DNA. Endogenous Cu can be found complexed in form of proteins such as ceruloplasmin which oxidises Fe(II) to Fe(III) so that latter can bind to transferrin to be distributed within the body.[44] Other Proteins containing Cu would be the ascorbate oxidase, the Cytochrome c

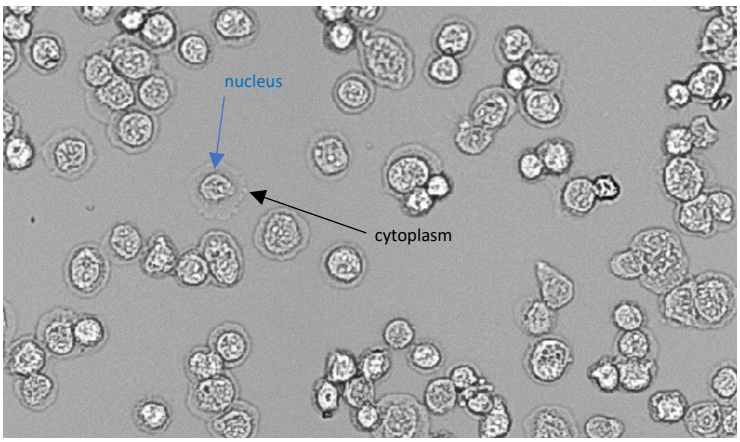

Figure 7: Microscope picture of a HaCaT sample showing cells and their boundaries between the cytoplasma (black) and the nucleus (blue). (the contrast of the image has been changed for demonstration pourpouses)

oxidase or the ethylen receptor. However, Cu stays a micronutrient.[45] This overlap shows that the ^{193}Ir-based segmentation is not considering the whole cell but rather just the nucleus or DNA. So, for the same cell segmented with both signals, the segmented area for the ^{63}Cu-signal is larger compared to the area segmented based on the ^{193}Ir-signal (Figure 8). The difference in dimension between the complete cell and the nucleus can already be seen under the microscope (Figure 7). The disadvantage here is, that not all of the marker present in the cell is considered, especially for the already in intensity low G1 and G2 markers when the segmentation is done based on the ^{193}Ir-signal. Furthermore, the information about the dimension of the cells as for example the area or diameter are lost. However, the advantage of the segmentation via Ir is, that this maker only stains the DNA within the cell and not the complete dimensions/cytoplasma of the cell. This facilitates the segmentation, because even though if two cells are touching each other, there DNA and thus the DNA-maker does not or just hardly touch each other. This facilitates the segmentation because the boundaries between the nuclei are more distinct compared to the cell's cytoplasm. This results in less mismatches and more suitable data.

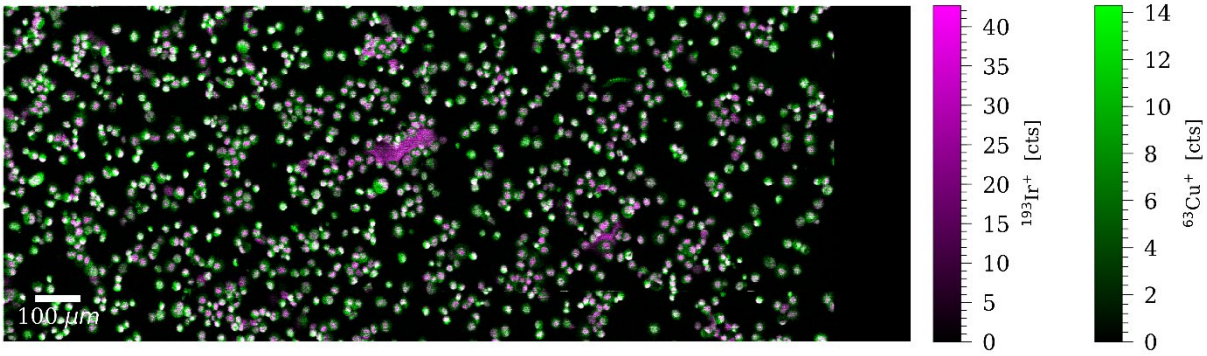

Figure 8: Overlap of the ^{63}Cu and ^{193}Ir signal from a taxol treated HaCaT sample showing the difference in area which will be segmented in further steps.

Basically, it depends on the information wanted (physical properties of the cells) and which segmentation method is used for what signal is used. When having dense cytospins as for example the A2780 samples, the segmentation based on the ^{63}Cu-signal can not be used as there are to many mismatches. The ^{193}Ir-signal can partly be used for the segmentation whereas there were still to many mismatches and duplicates. However, for less dense or optimal dense cytospins, both signals could theoretically be used. Also, a combination of both signals can be used depending on the segmentation program. The segmentation methods and the evaluation of the best method will be discussed in in the next sections of this work.

One possible method to stain the cells based one metal-based marker would be by using maleimido-mono-amide-DOTA (mDOTA) conjugated with a lanthanoid like ^{169}Tm. mDOTA

can bind free thiol groups like within cysteine and ultimately stains the whole cell.[46] The segmentation could thus be done based on a marker ant not based on an impurity.

4.1.6 Finding the optimal segmentation method

4.1.6.1 Introduction into the used software

Four different methods were tested for the segmentation of cells, showing each different advantages and disadvantages. The four segmentation methods are based on different principles. HDIP and CellProfiler are watershed-based algorithms. Ilastik is a machine learning based algorithm and cellpose a neural network with pretrained neural nets. When segmenting the sample with the different programs, different strengths and weaknesses of each method were revealed. For the selection of the best method for this works, focus is directed towards the usability of the resulting segmentation data (e.g. number of mismatches or biological information which can be extracted from the data); customizability of the settable parameters; amount of segmentation steps; learning curve/time needed to become proficient at using the segmentation software/algorithm; time needed for segmentation itself as well as which cytospins can be used with each program. The TIFF-files used for the segmentation and extraction of the data have been generated by HDIP. The input data for HDIP is the raw data received from the LA-ICP-TOFMS. These TIFF-files can be used for the segmentation within HDIP itself and CellProfiler. To use the data for Ilastik and cellpose, the ^{63}Cu and ^{193}Ir TIFF-files have to be merged into one multi-channel image. This can be done with CellProfiler although other, photography-based programs can also be used. For all segmentation methods, objects touching the edges have been removed within CellProfiler as they would falsify the data because cells touching the borders have not been fully ablated and would falsify the area or diameter. Only the HaCaT samples have been used for the selection of the best segmentation method for this work as the density of the cytospins is crucial for the selection of the segmentation method. The segmentation of the A2780 samples can for example not be performed up to date. Neither with the ^{63}Cu-signal, nor with the ^{193}Ir-signal. These samples are way too dense for the segmentation methods. For this reason, new, less dense cytospins with HaCaT cells have been made (part 4.1.3). For measuring the HaCaT samples the first time, Ilastik and cellpose were tested for the first time and immediately showed better results compared to HDIP and CellProfiler. The HaCaT control sample used within this part of the work has been ablated with a fluence of 1.5 J/cm^2 and overlapping spot size of 2 µm, resulting in 1 µm spots.

4.1.6.2 Watershed-based methods

HDIP:

For HDIP, there are many different settings which can be tuned for the segmentation. The most critical parameters were the minimum circularity, the minimum and maximum area as well as the maximum and minimum diameter. However, segmented cells showed holes within the segmented areas. This was partly solved by the inclusion of a dilation factor where one additional pixel around the segmented area is added. While this improved the segmented areas to be less patchy, more mismatches occurred, and fewer cells were segmented. In total, there are several steps and changes in the settings before segmentation can be done. The segmentation based on the ^{63}Cu- and ^{193}Ir-signal can not be done within the same run but must be performed and optimized separately. More settings were available, however these did not show a great effect on segmentation.

HDIP (Figure 10a) shows the smallest and fewest number of segmented objects (865), while also showing the greatest number of mismatches. For HDIP, to many mismatches occur when using the ^{63}Cu-signal for the segmentation. For this reason, the ^{193}Ir-signal must be used thus giving no information about the cell dimension. In Figure 11a, a cutout of Figure 10a, on the top right corner, there are two single cells which are not touching any other cells but have not been segmented. In the middle part of Figure 11a, there are several mismatches and duplicates. Once, four cells have been merged into one segmented object.

When it comes to the time needed for the segmentation, HDIP is overall the fastest method (several minutes) when it comes to the segmentation as there are only a few settings which must be optimized. Because there is no algorithm which has to be trained, no time additional time is needed before the final segmentation. However, the software is slightly buggy and crashed several times. No additional program is needed for the data extraction. One advantage of HDIP (and cellpose) is, that the signal can be overlapped with the segmented area. This enables to directly see which cells have not been segmented at all or incorrectly. For CellProfiler and Ilastik, this is not possible and complicates to check the data for bad segmentation.

CellProfiler:

For CellProfiler, many different packages can be chosen. The packages used for the preparation of the segmentation were to rescale and smooth the intensity, to identify or segment the cells and to measure the cells parameters and intensities of the markers. When it comes to the total

steps needed for segmentation, it depends if the pipeline has to be set up which would be many steps compared to if the pipeline is already finished. The setup and optimization of the segmentation pipeline needs longer (30 – 60 minutes) no template is available. However once set up, the segmentation is very fast with less than a minute needed for the segmentation itself. From a subjective point of view, CellProfiler is the hardest method to optimize for a proper segmentation as it is not very intuitive.

For CellProfiler, to many mismatches occur when using the ^{63}Cu-signal for the segmentation. For this reason, the ^{193}Ir-signal must be used thus giving no information about the cell dimension. When having optimally dense cytospins, segmentation based on the ^{63}Cu- and ^{193}Ir-signal can be done within the same run. CellProfiler (Figure 10b and Figure 11b) shows a few mismatches for example when cells get to close to each other (in the middle of Figure 11b) but nearly any signal has not be segmented at all which was the case for HDIP. Thus, CellProfiler shows already a huge improvement over HDIP. When segmentation is done with CellProfiler, no further program has to be used for data extraction.

4.1.6.3 Random forest classifier and neural net-based segmentation method

Ilastik:

Ilastik works differently compared to HDIP and CellProfiler. Within the random forest classifier, the background, the cytoplasma (^{63}Cu) and nuclei (^{193}Ir) must be manually drawn into the image or for some part of the image. These annotations are implemented into the algorithm. Areas with a high uncertainty, so falsely segmented areas where the annotation of multiple labels overlap, are ideally reduced by training the algorithm. Through adjusting the annotations, the training data is changed which leads to a different segmentation according to our changes. For HDIP and CellProfiler, the segmentation algorithm can also be manipulated by changing the hyperparameters of the segmentation procedure. Within Ilastik, either the algorithm is trained for each measurement, or a previously trained algorithm can be used. The segmentation based on the ^{63}Cu- and ^{193}Ir-signal are done within the same run. For this reason, no data is lost about the cells dimension which is an important advantage over HDIP and CellProfiler where the ^{63}Cu signal shows to many mismatches to use. Segmentation based on Ilastik (Figure 10c and Figure 11c) shows that there are still several mismatches and multiplicates but already less than HDIP but more compared to CellProfiler (if ^{193}Ir-signal

used). In the middle of Figure 11c are several duplicates and one quadruplicate (four cells in one segmented object.

The training of the algorithm for Ilastik for one sample takes about 20 minutes for an image such as Figure 10c. When training the algorithm based on several samples, the time needed stacks up. However, the segmentation can also be done for smaller sections of the image and the trained algorithm be applied onto the complete image. This reduces the time needed for the training of the algorithm whereas less data is used for the training of the algorithm. After the segmentation with Ilastik, Cellprofiler must be used for the extraction of the single cell data.

Cellpose:

For the segmentation via cellpose, a pretrained neural net has been used. Cellpose offers a *model zoo* with several pretrained neural nets. The *cellpose nuclei model* showed the best result for the cytospins. As for Ilastik, the segmentation is done based on a combination of the ^{63}Cu- and ^{193}Ir-signal. After the first segmentation with a pretrained algorithm, the user can manually correct the outlines of the cells. Duplicates and mismatches can be identified by overlaying the segmented areas with the ^{193}Ir signal. The nuclei signal for two cells are more separated compared to the signal originating from the cytoplasm. Therefore, duplicates can be easier identified when comparing the segmented area with the ^{193}Ir-signal (Figure 9c) compared to the ^{63}Cu-signal (Figure 9b). For this reason, the nucleus-signal highlights duplicates and mismatches which then can be corrected manually by the user (Figure 9).

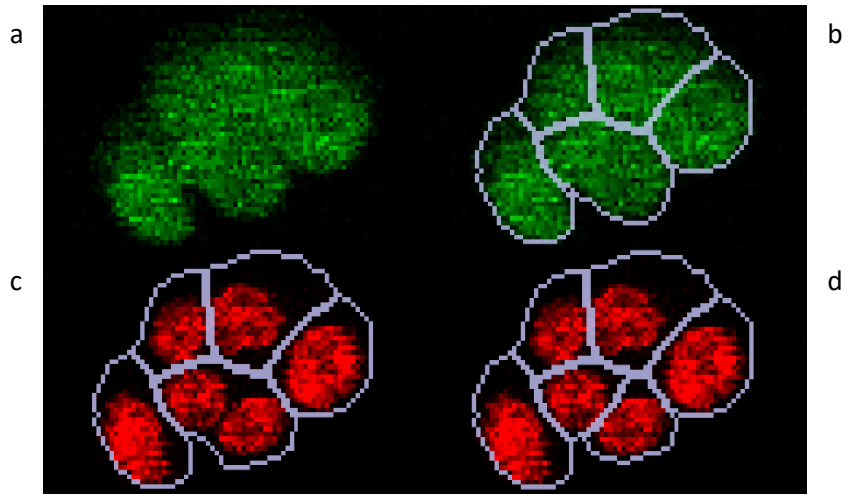

Figure 9: All the images a-d are the same HaCaT control sample. In green is the ^{63}Cu-signal, in red the ^{193}Ir-signal and the white encircled areas are the segmented objects. a shows the raw ^{63}Cu signal where no differentiation between all the cells can be seen. b shows the segmentation area overlapped with the segmented areas resulting in five cells. c shows the overlap of the ^{193}Ir-signal and the segmented area revealing six nuclei in 5 segmented areas. Thus one duplicate was revealed. d shows the overlap of the manualy redrawn/corrected segmented area with the ^{193}Ir-signal resulting in six segmented areas with six nuclei.

The newly, manually corrected dataset then can be used to retrain the neural network in order to improve it. In this work, cellpose uses both signals simultaneously for the segmentation whereas single channel (nucleus or cytoplasme) segmentation can also be performed. However, segmentation based on the two signals gives the most reliable data for this samples when it comes to overall segmentation, mismatches, and dimension of the cell.

The nucleus neural network used for cellpose has been retrained based on six different HaCaT-samples. The algorithm could not be trained with the A2780 samples as they were too dense and there would have been to many mismatches and duplicates been implemented into the retaining leading to an even worse segmentation. The retraining of the neural net algorithm takes the longest compared to the other methods as after each training, the complete image has to be checked for mismatches and duplicates. However, cellpose also shows the best results.

Cellpose (Figure 10d and Figure 11d) shows the biggest segmented areas, the highest number of objects (1064) and the least mismatches. the segmentation based on cellpose seems to be the most accurate one as it also does not segment the cells based on the ^{193}Ir-signal but based on the ^{63}Cu-signal in combination with ^{193}Ir-signal. This is also the reason for the bigger areas when segmenting with cellpose. In Figure 11d, only one duplicate could be spotted.

Segmentation masks and table:

In Figure 10 are the segmentation mask for HDIP (a), CellProfiler (b), Ilastik (c) and cellpose (d) for the same HaCat control sample.In Table *5* are the total number of segmented valid cells (cells not touching the boarder) as well as the number of cells removed.

Table 5: Total number of cells removed and segmented for HDIP, CellProfiler, Ilastik and cellpose from the HaCaT control sample to compare the different segmentation methods.

Taxol:	Cells removed	Segmented valid cells
HDIP[1]	No data given[3]	865
CellProfiler[1]	53	1007
Ilastik[2]	69	964
cellpose	67	1064

[1]For this method, the ^{193}Ir-signal was used. [2]Was this method, a combination of the ^{63}Cu and ^{193}Ir signal was used. [3]The data was extracted by HDIP and not CellProfiler. HDIP does not give the number of removed objects.

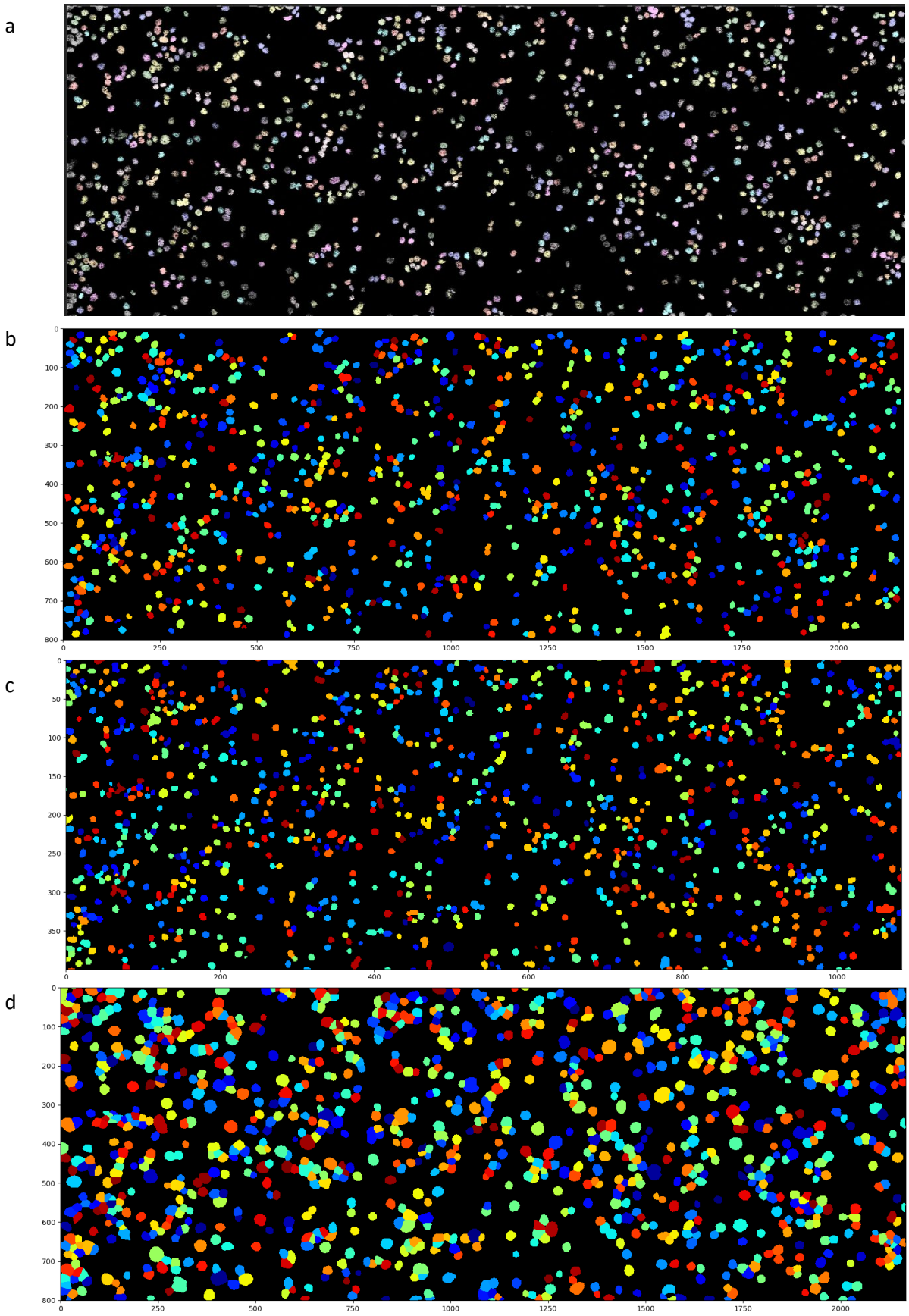

Figure 10: Comparison of the segmentation of a control sample based on different segmentation methods. HDIP (a) and CellProfiler (b) have been segmented based on the ^{193}Ir signal whereas for Ilastik (c) and cellpose (d), the segmentation itself was done based multi-channel images incorporating the ^{63}Cu- and ^{193}Ir-signal.

4.1.6.4 Conclusion

The segmentation based on cellpose seems to be the most accurate one as it also does not segment the cells based on the ^{193}Ir-signal but based on the ^{63}Cu-signal in combination with ^{193}Ir-signal and shows the least mismatches. However, the retraining of the neural network took the longest as preparation for the segmentation compared to the other methods. Once the pipeline is set up, the segmentation works excellent and takes less than a minute. Whereas checking for mismatches within the cellpose segmentation is recommended as mismatches are not impossible and improves the data even further. Measuring physical parameters of the cells like the mean area and diameter of the cells which can not be done when segmentation is only done based on the ^{193}Ir-signal. Cellpose is the most user-friendly program of all of them and enables to directly correct wrongly segmented cells which must be done with any of the other methods.

If the user wants a rough and fast inside into the results of new samples, CellProfiler is the go-to program. However, as previously explained, the segmentation results are inferior to cellpose and there are still to many mismatches for publishable data even though the method is the fastest segmentation method with usable data.

Within CellProffiler, there are many different measurements which can be exported like for example the mean, median, integrated, max, min, UpperQuartile, LowerQuartile intensity and even more. This are only the examples for the intensities which are extractable. This can not be done within HDIP.

For a proper conclusion, the cells being ablated should be counted manually on the respective microscope picture.

In Figure 11 are the same cutouts of the segmentation masks from the masks in Figure 10 to compare the different segmentation methods. This cutout has been chosen, as there are several free cells whereas there is also one region where cells are closer to each other showing the problems with mismatches and duplicates for denser cell regions.

	Time for training/setting up the pipeline [min]	Segmentation result	usability of the data	Signal input giving reasonable data	Additional data
HDIP	5	bad	medium	^{193}Ir	/
CellProfiler	depending on the sample [1]	medium	difficult	^{193}Ir	/
Ilastik	20	medium	easy	^{63}Cu + ^{193}Ir	Cell physics
Cellpose	30	excellent	easy	^{63}Cu + ^{193}Ir	Cell physics

[1]As the settings for Cellprofiler are not as intuitive compared to the other methods, there must be tried out more different settings and no general timescale can be defined.

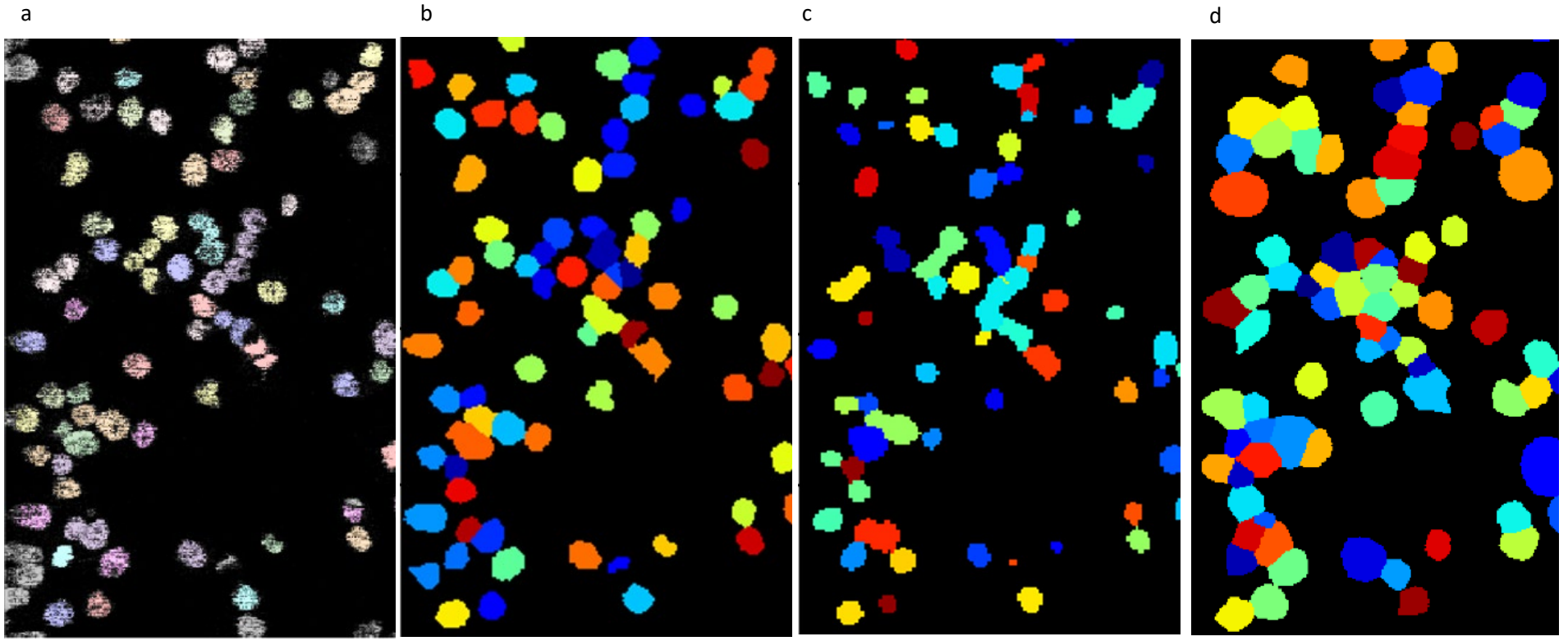

Figure 11: Zoomed image of the segmentation masks for the HaCaT control sample. a: HDIP; b; CellProfiler; c: Ilastik; d: cellpose

4.2 Staining and its challenges

The staining of IdU is done by the Medical University of Vienna and is done after the treatment of the samples. The IdU staining optimization was already previously explained in part 4.1.4. The staining with the ^{193}Ir-intercalator and the metal tagged antibodies is done after the fixation of the cells on the cytospins. The staining procedure consists of several steps including washing, permeabilization, staining and blocking steps which can be optimized. For example, different permeabilization methods can be used. For the A2780 samples, Triton^{TM} X-100 was used whereas Tween was used for the HaCaT samples. A comparison between the different permeabilization reagents can not be made as different cell lines have different properties. However, Tween was more convenient to use. A blocking solution like BSA is used to block unspecific binding sites to reduce the unspecific binding of the markers which would lead to higher background signals within the cells. The staining time, the concentration and temperature during the staining are crucial for the actual staining step. For the A2780 samples, all metal labeled antibodies have been used with a dilution of 1:100 and the staining was done at 4°C overnight. For the HaCaT samples, the dilution of the G1- and G2-marker was increased to a dilution of 1:50 to increase the marker intensity as both gave rather low signal intensities. The staining temperature and duration was not changed as well as the M-phase marker dilution. For the two optimization attempts for the staining of the G1- and G2-marker once the dilution was changed from 1:50 to 1:200 and once the staining time and temperature was changed from 4°C overnight to 30 minutes at room temperature. This is going to be explained in part 4.3.6

4.3 Challenges

The validation of the data comes with several challenges which must be overcome. Firstly, as already explained, cancer cells are disturbed within their cell cycle homeostasis. This can have different origins like for examples the depletion of the Rb protein leading to no cell cycle arrest in G1 if needed and progression into the S-phase[47] or to bypass the mechanisms which induce apoptosis.[48] Within this work, healthy immortalized keratinocytes (HaCaT cell line) have been used as well as human ovarian cancer cells (A2780 cell line). Secondly, the specificity of the antibodies is key for a proper staining. Too much unspecific binding leads to an overlapping of the background signal with the marker signal within the cells and thus gives non-usable data. Unspecific antibodies lead to wrong data. The pRb-protein is present during mostly the complete cell cycle. However, there are 13 different phosphorylation patterns known for the Rb-protein each of them resulting in different conformations and functions of the Rb-protein. The antibodie for the actual anti-pRb [Ser807/811] protein might have a small affinity to the other conformations. Additionally, several CDKs and cyclins are not present in the same concentration during the complete cell cycle phase. Some CDKs or cyclins like cyclin B1 build up during the progression though the cell cycle. Thus, the concentration can differ in the early and late stage of a phase or can also be present in more than just one phase (part 4.3.4). This is also one problem leading to the third challenge, the thresholding. Thresholding is important as wrongly placed thresholds will lead to wrong cell cycle phase attributions leading to corrupted data. Poor or insufficient staining leads to thresholding problems ass the differentiation between two populations blur (part 4.3.1). Fourthly, a proper segmentation is necessary to get single cell data which is the aim of the work.

All the following data has been obtained by using miniconda with the cellpose environment for the segmentation, CellProfiler for the extraction of the data and R for the statistical analysis. As a showcase model, two HaCaT samples has been used with once no special treatment (Control sample) and once a taxol treated sample. For the control sample, the antibody droplet broke through the PAP pen. Whereas the cells were still covered in liquid. For this reason, the sample has not been redone as the markers later described look good. The segmentation was done based on the ^{63}Cu-signal as primary dataset and the ^{193}Ir-signal as secondary dataset. The “nuclei” basic segmentation algorithm has been used and was optimized based on four differently treated HaCaT samples as well as two more HaCaT control samples. The optimization of the algorithm has been done by correcting mismatched cells or poorly segmented cells by redrawing the outer dimensions of the cells. These data sets have then been used to implement and train the new

segmentation algorithms. After saving the corrected masks for each sample, the files have been processed in R in order to remove the cells touching the borders. These are uncompleted, not-fully segmented or ablated cells and would corrupt the final data like for example the mean area or diameter. The segmentation of the control sample of the HaCaT cellline with cells touching the borders being removed is showcased in Figure 12. In total, 1046 cells have been detected not touching the border. The number of cells being removed, and total number of intact cells being segmented are listed up in Table 6 for all the four treatments. For all the samples, approximately the same area has been ablated and the number of cells per measurement was in the same range. Thus, the segmentation was similar for all the samples. The number of cells segmented reaches from 1034 cell for the cisplatin treated sample to 1175 for the taxol treated sample. All the segmentation masks are in illustrated in Appendix 3.

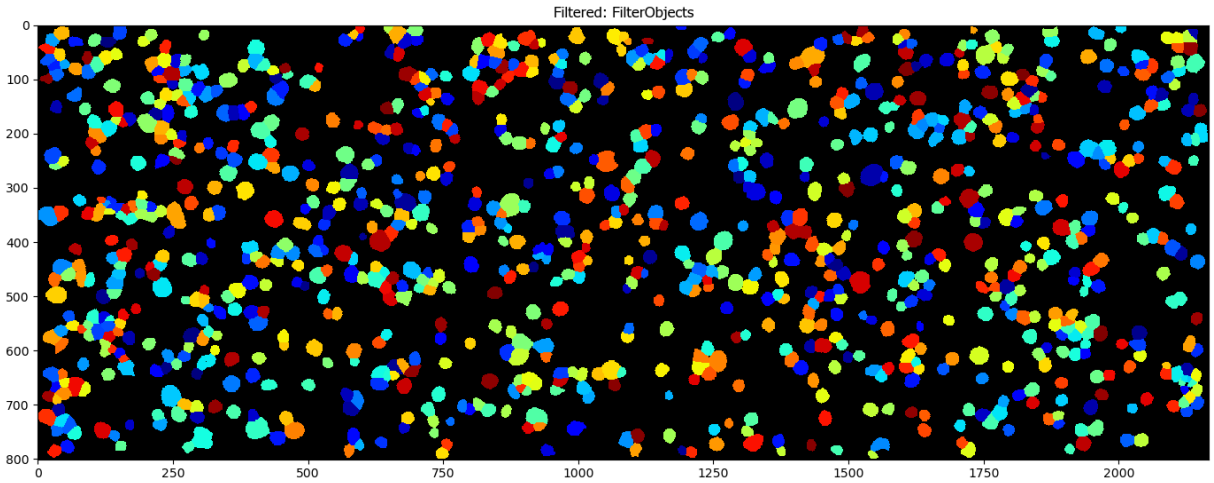

Figure 12: Segmentation of HaCaT_CtrC_rep1_1um with cells touching the borders removed (1046 cells detected).

Table 6: List of cells being removed for each four differently treated sample as well as the final amount of segmented cells. Segmentation was made based on cellpose.

Taxol:	Cells removed	Segmented cells
Control	67	1046
0% Serum	42	1144
Cisplatin	73	1034
Taxol	67	1175

4.3.1 Thresholding and its problems

Thresholding is the biggest problem in the evaluation of the data as it is very subjective. All the data used for the formation of the point plots has been normalized by the area of the cells. According to literature, one way to set thresholds for segmentation is by including expert

knowledge and thus setting expert-defined thresholds.[49] There is no mathematical thresholding method known for this problem which could be implemented into this evaluation and give reasonable data. So, one possibility of thresholding is by making point plots where the desired marker intensity of each cell is plotted against its respective ^{193}Ir-signal (Figure 13) as every cell should have incorporated some of the DNA intercalator. Thresholds are set by the visual distinguishment between two populations or by placing it near a difference in density of the number of cells in the marker intensity. When there is no clear difference between the two population, small differences in setting the threshold can have a huge impact on the final evaluation. This was the case for the G1- and G2-phase and is going to be explained in part 4.3.4 and 4.3.5. In Figure 13 are two point plots illustrated which show once no real separation of two populations for the G1 marker (a: HaCaT taxol treated sample) where it is difficult to set a proper threshold and once a point plot where two populations can be identified (b: HaCaT taxol treated sample) where the setting of the threshold is rather obvious. The thresholds set represent the blue line. The cells on the left side of the threshold (blue line) are seen as background signal and unspecific binding. The cells on the right side of the threshold are attributed to the respective cell cycle phase according to the principle of exclosure. One other problem is that the thresholds can heavily depend on the treatment. So depending on the treatment, different thresholds have to be set for the same marker. For this reason, no overall threshold can be set which fits for all the treatments for the same phase. This was especially the case for the S-phase which I explained in part 4.3.3.

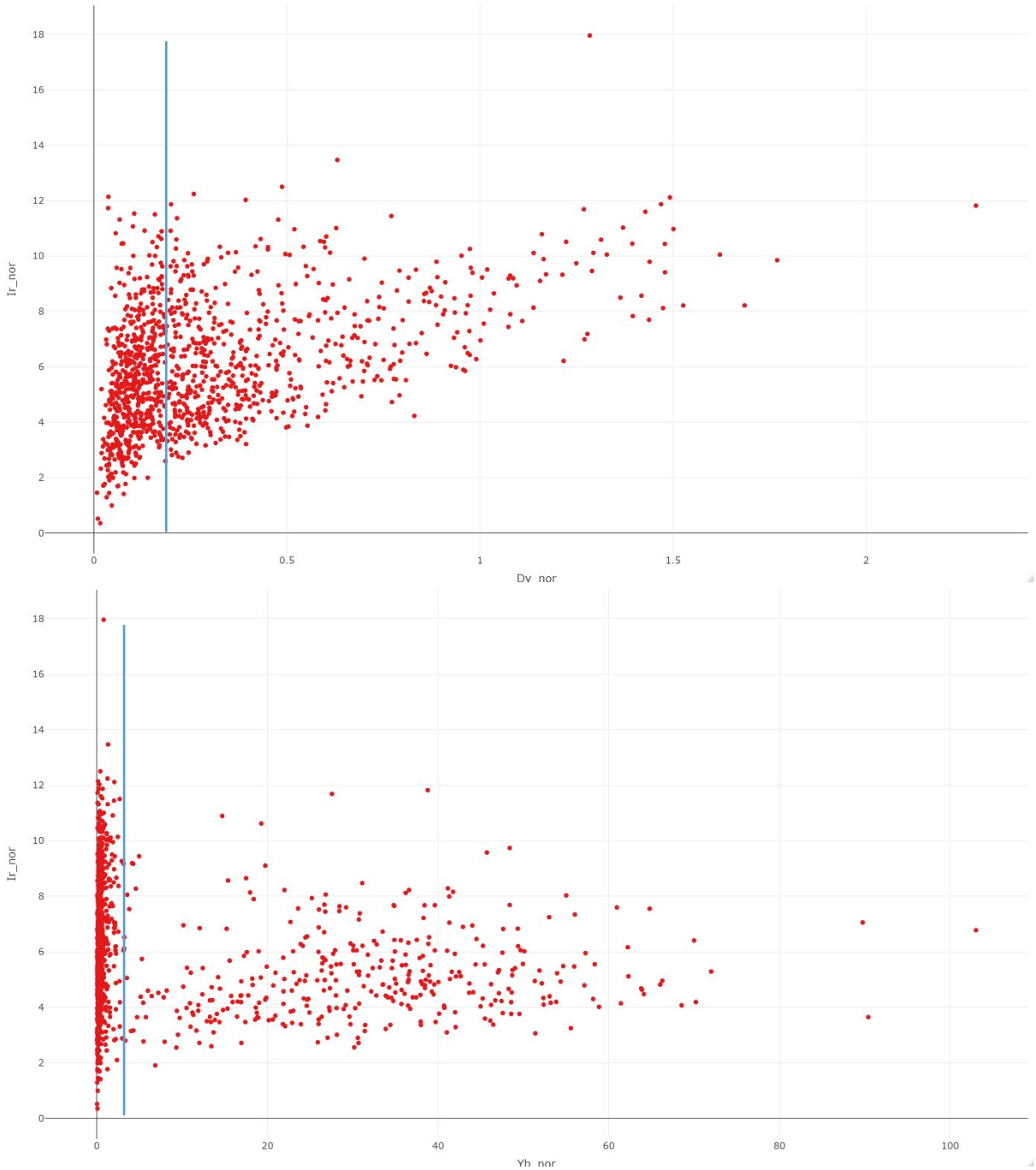

Figure 13: Point plot of the normalized G2- (a) and M-phase (b) marker signal against the normalized ^{193}Ir signal for the HaCaT taxol treated sample showing the problem of thresholding when no two populations can be identified (a) or when proper thresholding can be done due to to populations.

4.3.2 M-phase

The M-phase marker is binding to the phosphorylated H3 histones which are responsible for the winding up of the DNA and is only found during the M-phase.[36] In the attribution process of the different phases, the M-phase is the first one to be set as the marker is said to be very specific. This is also confirmed when analyzing the point plots (Figure 14b). Only a few cells show extremely high signals which are cells in the M-phase. The marker did not need any optimization as cells being in the M-phase can clearly be separated from the background noise and the other cells. Thresholding was thus no problem. The only optimization which could be implemented in further analysis is to reduce the amount of marker used to cut the cost for each measurement. The current dilution of the M-phase marker is 1:100. The taxol treated sample shows a fragment originating from the LA-ICP-TOFMS data on the right side of the image (Figure 14a).

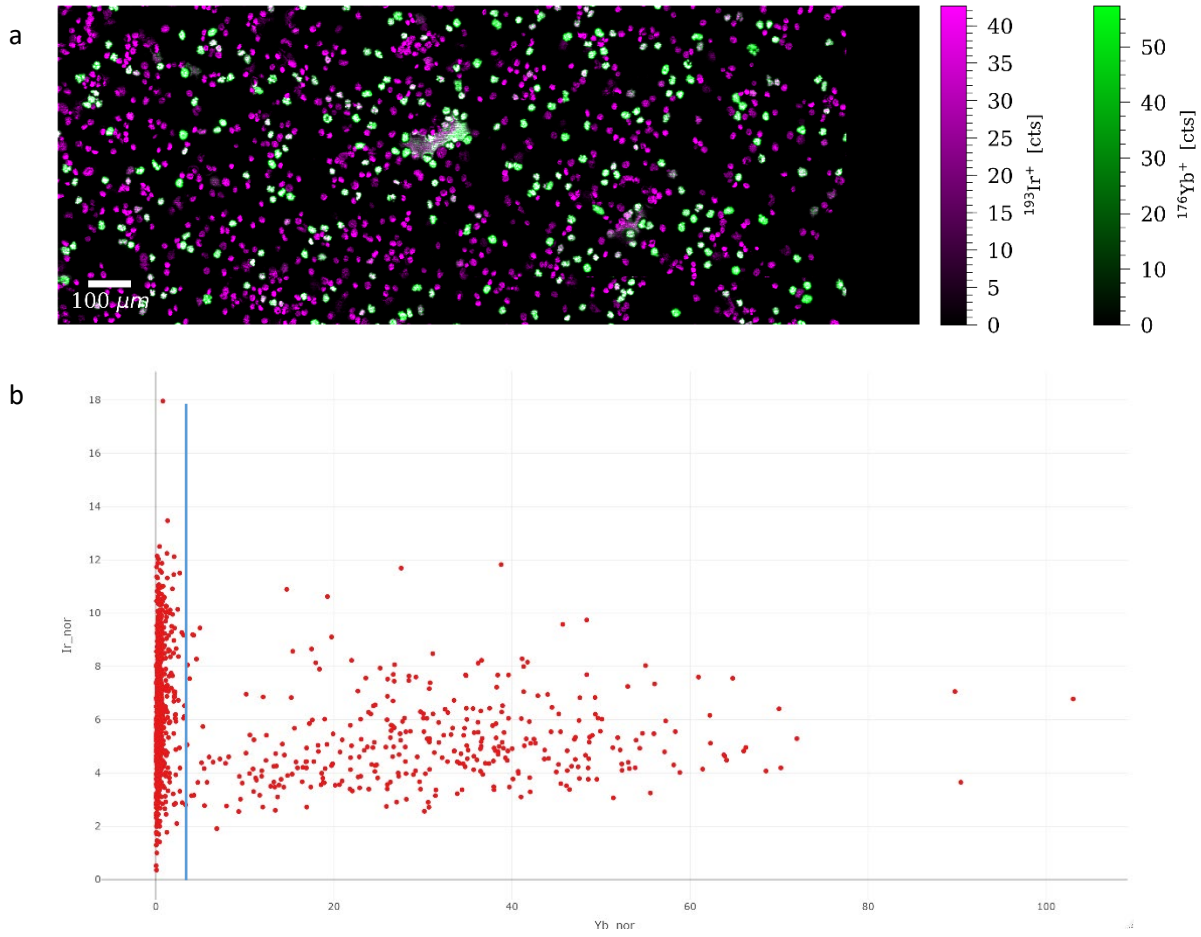

Figure 14: a: Overlap of the raw images from HDIP of the ^{193}Ir and ^{176}Yb signal for the taxol treated HaCaT sample. b: Point plot (^{193}Ir-intensity vs ^{176}Yb-intensity) of the same taxol treated HaCaT sample showing two separate populations and the threshold set (blue line)

4.3.3 S-phase

The S-phase signal originally originating from the cell ID IdU shows a very high overall background signal not only within the cells, but rather all over the ablated area. This was already indirectly solved and discussed in part 4.1.4. This change of the incubation time from 30 to 60 minutes enabled the differentiation between two populations in the point plots (Figure 15). This increase in signal intensity leads to a separation within the point plots for the thresholding for the cell cycle gating. However, there can also be observed a difference in the point plots used for the thresholding of the four differently treated HaCaT samples. The 0% serum sample shows a higher background signal within the cells compared to the control, taxol and cisplatin sample. Figure 15 shows the HaCaT samples being incubated with taxol (a) and 0% serum (b) where the normalized S-phase marker signal is plotted against the normalized DNA intercalator signal. Here can clearly be seen a difference between the intensities between the two populations. The 0% serum sample shows a higher background signal for the S-phase marker compared to the taxol sample. The threshold set for the taxol sample is 11.5 CPS/pixel whereas the threshold for the S-phase for the 0% serum sample is 15.5 CPS/pixel. Thus, different thresholds must be set, and no global threshold can be set for different sample even though they are the same cell culture and just differently treated (0% serum instead of taxol). This shows that the treatment of the cells has somehow an influence on the uptake of the marker. One possibility for this would be that the cells within the 0% serum sample are starving during the cultivation which should arrest them in the G1- and S-phase. When cells are starving, they might take up more of the nutrients that are available in the medium. The only nutrient available in the medium in this case is the IdU. Thus, all cells might take up more of the IdU which is stored in the cell leading to a higher ^{127}I-background for the cells. Whereas also cells which are in the S-phase have stored more of the IdU in the cell additional to the IdU which has been incorporated into the DNA. Thresholding can still be done as the two populations are distinguishable. The staining with IdU is very specific as the S-phase is the only phase in which IdU is heavily incorporated into the DNA. In G1 and G2, the DNA is getting checked and repaired in case of DNA damage. This is another possibility of IdU getting incorporated into the DNA. However, this incorporation of the IdU is minor compared to the incorporation during the duplication of the DNA in the S-phase. To conclude, the staining with IdU works well to track down the S-phase.

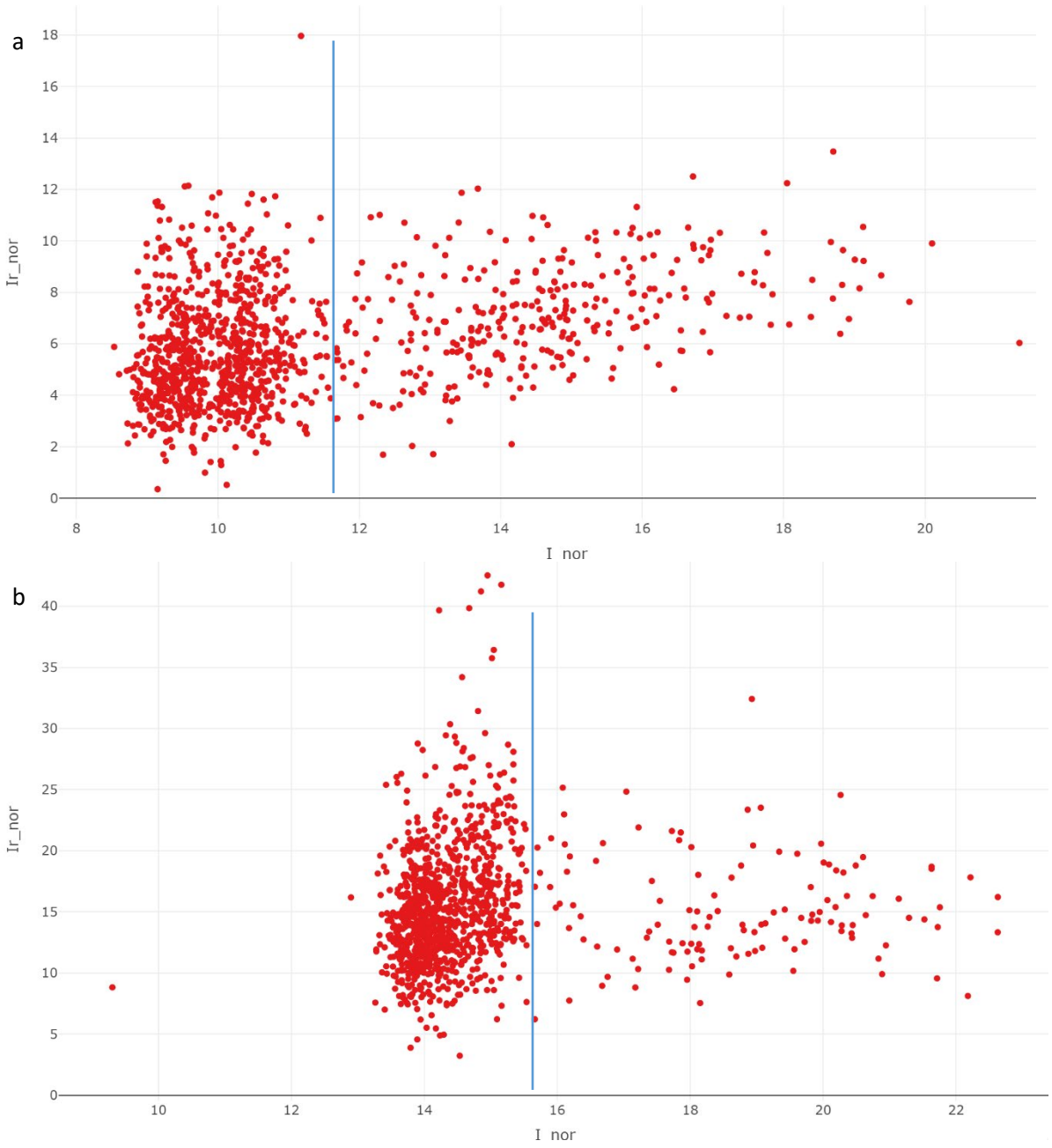

Figure 15: Point plots of the taxol (a) and 0% serum (b) sample where thenormalized ^{193}Ir-signal is plotted against the normalized ^{127}I-signal to compare the difference in threshold for the same cell culture treated differently.

For the cisplatin treated sample, the iodine background changed at the end of the measurement (Figure 16). This leads to the problem, that the cells which are ablated at the end of the measurement will be lower in intensity as the impurity adds up to the total signal intensity. Thus, the cells on the lower hand of the image have about the same intensity as the background signal from the rest of the measurement. These cells will thus be below the threshold which leads to corrupted data. This measurement must be redone. Somehow the iodine background was removed. How this was possible is not known.

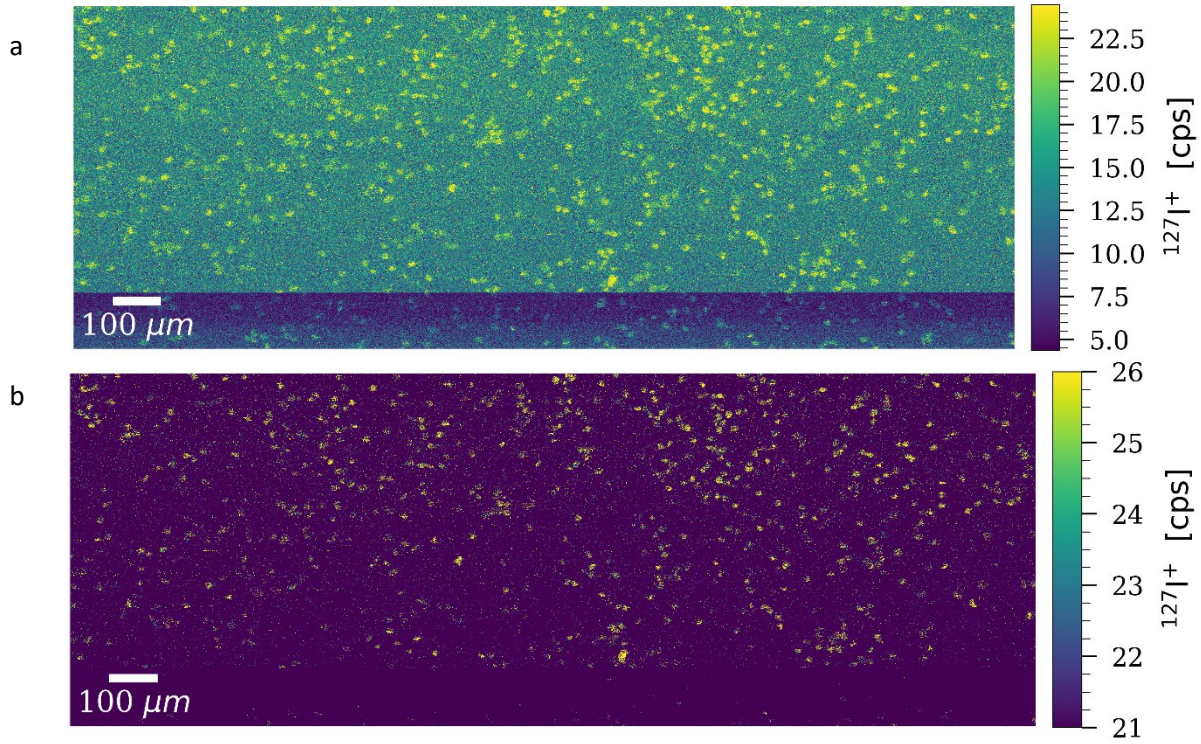

Figure 16: ^{127}I raw signal extracted from HDIP for the cisplatin treated sample showing an uneven background at the bottom (a) ^{127}I signal extracted from HDIP for the cisplatin treated sample showing when adapting the scalebar, the ^{127}I signal within the cells disappears (b).

4.3.4 G2-phase

The third phase assigned is the G2-phase by tagging cyclin B1. Here some problems appeared. First, the overall ^{164}Dy-signal intensities are extremely low compared to the S- and M-phase. The most intense signal for a cell showing the G2-marker is 2.3 CPS/pixel compared to 21 CPS/pixel for the S-phase and 103 CPS/pixel for the M-phase for the respective marker within the taxol treated sample. This might be since regulating and signaling proteins are mostly less abundant proteins compared to structural and functional proteins[50] like the histone proteins or IdU which is heavily incorporated during the replication of DNA during the S-phase. However, the staining with the marker is not quantitative but rather qualitative. Both markers might naturally come in higher concentrations compared to the cyclin B1. The cyclin B1 content in the cells rises during the G2-phase until it reaches a peak in the late G2- and M-phase and rapidly declines in the metaphase or near the metaphase within the M-phase.[31c] This gradual increase in the cyclin B1 content within the progression from the S-phase to the G2-phase might leads to cells containing different amounts of cyclin B1 which by itself leads to a gradual distribution of the cells within the point plot. This is also observable when creating the point plot (Figure 17) by plotting the normalized intensities of the DNA-marker against the

normalized G2-phase marker. There are no two separate populations observable but a transition from a densely packed population to a wider spread population.

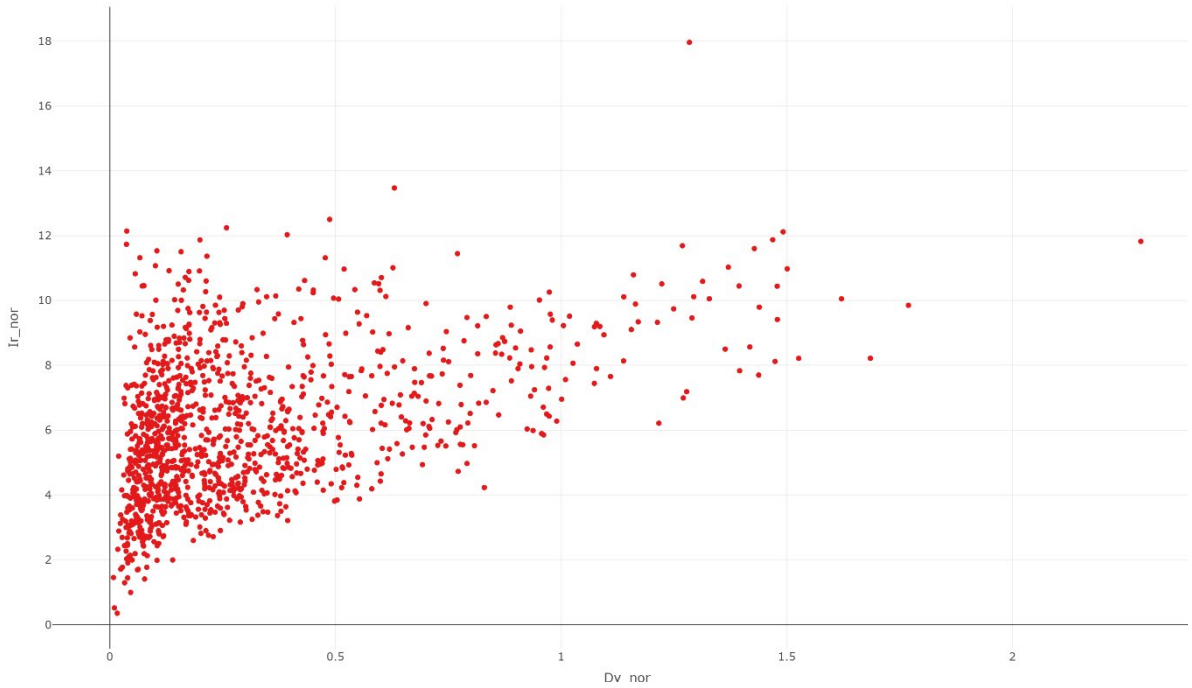

Figure 17: Point plot of the taxol treated HaCaT sample where the normalized intensities of the DNA-marker (^{193}Ir) and the G2-phase marker (^{164}Dy) showing no separation between two distinct populations but rather a gradual distribution of the marker intensity.

There can also be found an inconsistency of the specificity of the cyclin B1 in the different treatments. The overlap between the G2-marker and the S- or M-phase can be seen in Figure 18 for the control sample (a-b) and the taxol sample (c-d). Within the control sample, there is an overlap between the G2-phase marker and the S-phase marker (Figure 18a) whereas there is no overlap between the G2-phase marker and the M-phase marker (Figure 18b). The cells showing the most intense G2-marker signal are not cells within the M-phase for the control treated sample. For the taxol treated sample, there is an overlap between the G2-phase marker and the S-phase marker (Figure 18c) as well as for the M-phase marker (Figure 18d). To conclude, for the taxol sample, the cells showing the highest G2-marker signal are cells within the M-phase whereas this is not the case for the control sample.

For the cisplatin and 0% serum sample, the specificity of the G2 marker is different again. So, depending on the treatment of the cells, the specificity of the marker changes which can not be explained up to date. One possibility could be that the cells are manipulated though the treatment which might lead to a change of the cylcin B1 (same accounts for the pRb). Whereas no evidence can be found for this. A remeasurement of other technical replicates would be interesting to compare the data if these give the same results. Stokke et al showed, that the

cyclin B1 marker stains the late G2-phase as well as the M-phase. However, they used the anti-pLK1 marker for the differentiation between the late and early G2-phase in their work whereas they used the anti-Geminin marker to track down non G1-phase and thus attributed the G2-phase by the principle of exclosure.[5] So, they did not specifically track down a specific protein which is present in the G2-phase.

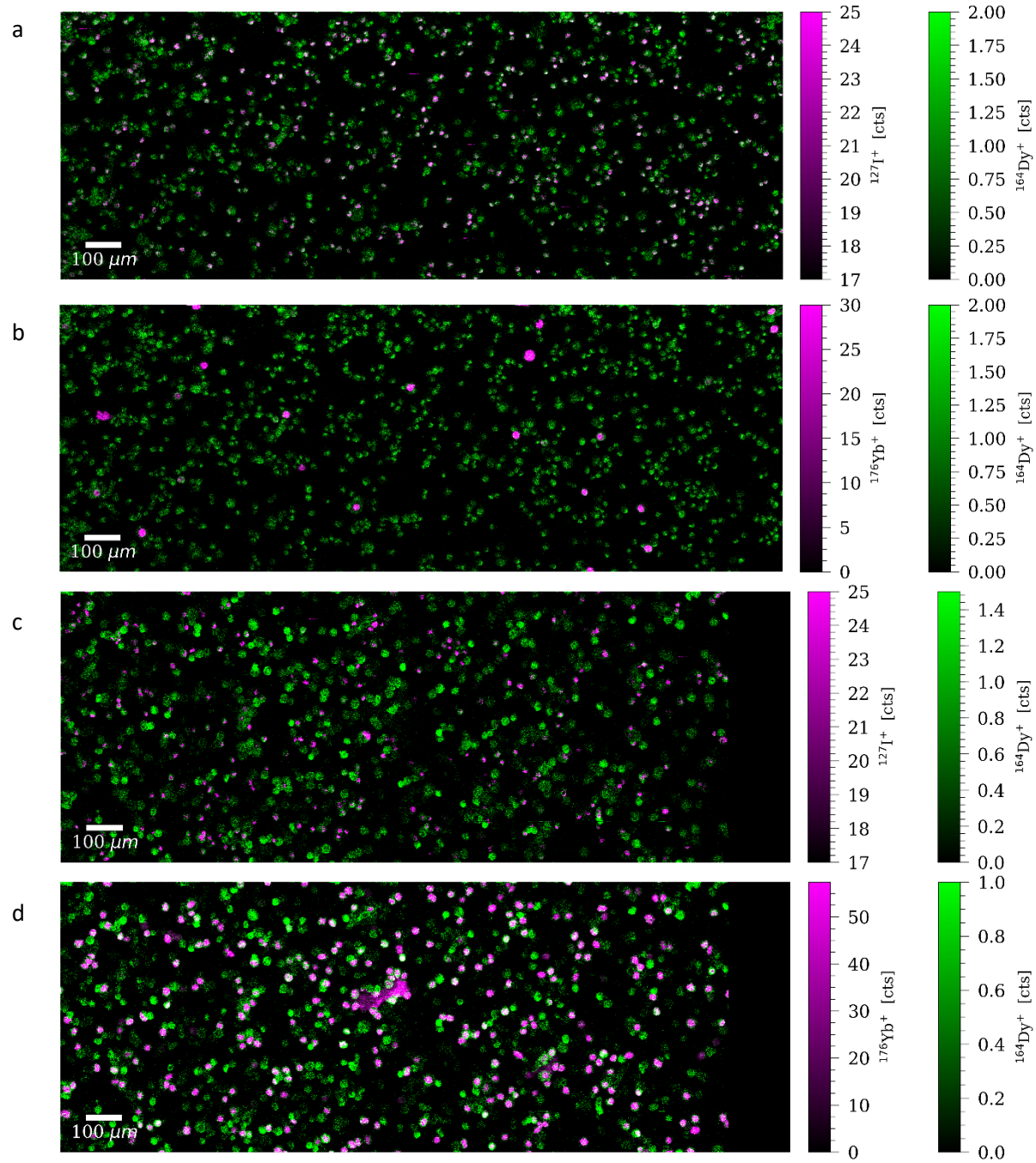

Figure 18: Overlaps of the G2 marker with S- and the M-phase marker for the taxol sample (a: $^{127}I/\ ^{164}Dy$; b: $^{176}Yb/^{164}Dy$) and the control sample (c: $^{127}I/\ ^{164}Dy$; d: $^{176}Yb/^{164}Dy$).

A previously said, the cisplatin treated cells should undergo mainly a S-phase arrest and partly a G1-phase arrest. This also fits the FACS data where no cells were in the M- or G2-phase

(Appendix 4). However, most cells in the cisplatin treated sample show the G2 marker whereas some are more intense (Figure 19). This reinforces the hypothesis of the cyclin B1-marker being unspecific as phase-marker. As described in the introduction, the cyclinB1 levels start increasing in the middle of the S-phase and continuously increase until reaching a peak in the M-phase which than rapidly decreases. The cells in the M-phase also show the G2-marker (Figure 19b).

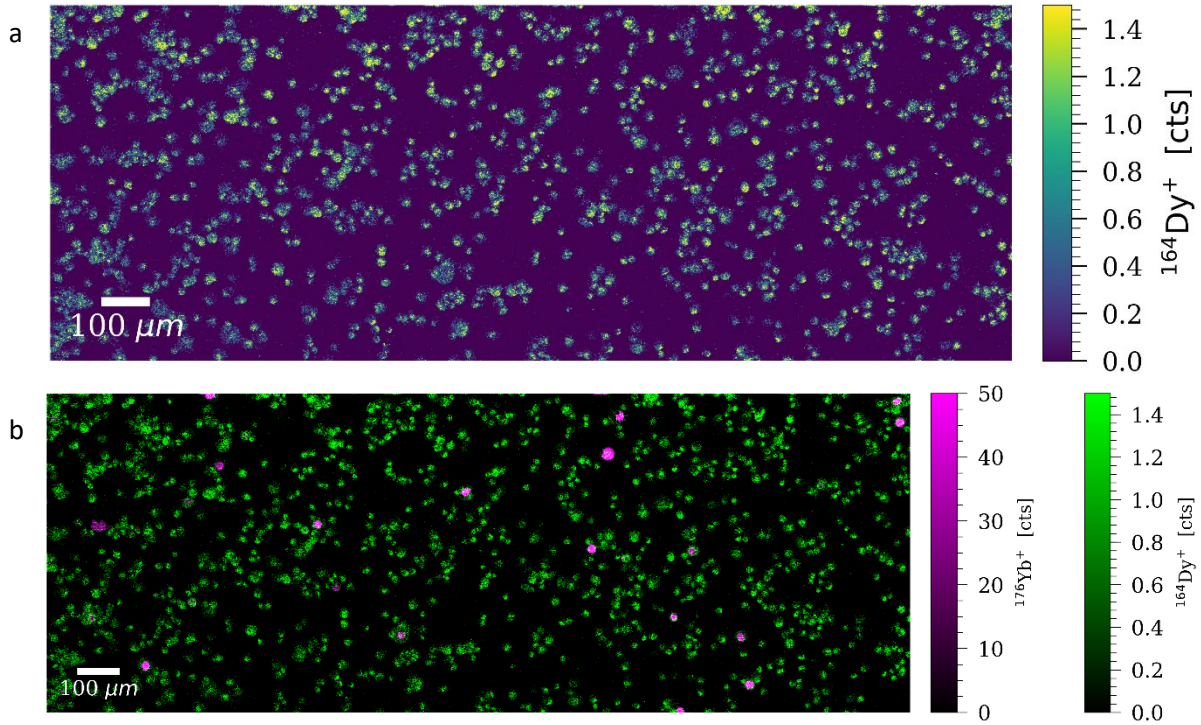

Figure 19: raw Data of the ^{164}Dy-signal for the cisplatin treated sample showing that cells have the G2 marker even though no or just a few cells should be in the G2-phase. (a) Overlap of the ^{193}Ir and ^{164}Dy-signal for the cisplatin treated sample showing that cells in the M phase also contain the G2 marker.

When calculating the normalized mean cyclin B1 signal intensity for each sample, the control and cisplatin treated sample show the highest mean value whereas the 0% serum sample the lowest. The taxol treated sample, which should arrest most of the cells in the G2 and M phase, shows less of the marker compared to the control and cisplatin treated sample even though both treatments arrest fewer cells in the G2- and the M-phase. Theoretically, if the cyclin B1 is expressed most in the G2- and M-phase, the taxol treated sample should show the highest cyclin B1 signal.

Table 7: List of the normalized and non-normalized signal intensities for the cyclin B1 for all the cells within the four differently treated samples.

	Normalized mean cyclin B1 intensity [cps/area of the cell]	mean cyclin B1 intensity per Cell [cps]
Taxol	0,305	166,759
Cisplatin	0,375	169,542
Serum	0,094	40,124
Control	0,399	179,563

If the cyclin levels are compared on a cell cycle phase basis for the different treatments, the cells in the M-phase show by far the highest signal intensities within the cisplatin treated sample. Within the control and taxol treated sample, cells in the cells in the G2-phase show the highest signal intensities whereas in the cisplatin and 0% serum sample, it's vice versa. Whereas only four cells have been in the M-phase for the cisplatin treated sample and two for the 0% serum sample. The G2-signal signal intensities in the 0% serum sample were generally lower compared to the other samples. However, this increase in cyclin B1 during the cell cycle progression and reaching its peak in the G2- and M-phase according to literature[31c] can also be seen within these measurements. Here must be considered, that the staining is rather qualitative and not quantitative.

Table 8: List of normalized mean cyclin B1 intensity per pixel for each phase in the four treatments.

	Normalized mean Cyclin B1 intensity per pixel for each phase in the different cell cycle phases [cps/pixel]			
	Taxol	Cisplatin	Serum	Control
M	0,391	**1,491**	**0,280**	0,455
G2	**0,750**	0,630	0,198	**0,762**
S	0,269	0,368	0,186	0,431
G1	0,148	0,254	0,071	0,412
G0	0,091	0,225	0,062	0,311

As already explained in the introduction, the cylcin B1 is shuttled into the nucleus at the beginning of the mitosis.[31a] When segmentation data based on ^{63}Cu and ^{193}Ir could be fitted together, this might enable a better cell cycle gating. As the cyclin B1 concentration is the highest in the M-phase and theoretically only present in the nucleus, this could be used for the data processing to improve the G2-phase attribution. To conclude, G2-phase attribution is not possible up to date.

4.3.5 G1-phase

The G1-phase is the last cell cycle phase attributed within the cell cycle gating strategy. As the assignment of the G2-phase is not fully optimized yet, the data about the G1-phase is not reliable. The signal for the G1 marker is present in mostly all the A2780 and HaCaT cells at very low intensities compared to the S- and M-phase marker. Either the cells are all in the G1-phase, the marked pRb-protein is present in all cell cycle phases or there is too much unspecific binding of the marker. All three of them would explain the uniformly low intensities of markers measured (Figure 21a). However, several cells can be spotted showing more intense signals. When overlapping the G1- and M-phase marker, it is obvious, that the cells with the most intense signal for the G1-marker are cells within the M-phase. This can be observed in the overlaps of the G1-marker with the M-marker (Figure 21b-c) or within the point plots where both signals are plotted against each other (Figure 20). Thus, the G1-marker stains the M-phase cells the most. This is true for the four different treated samples.

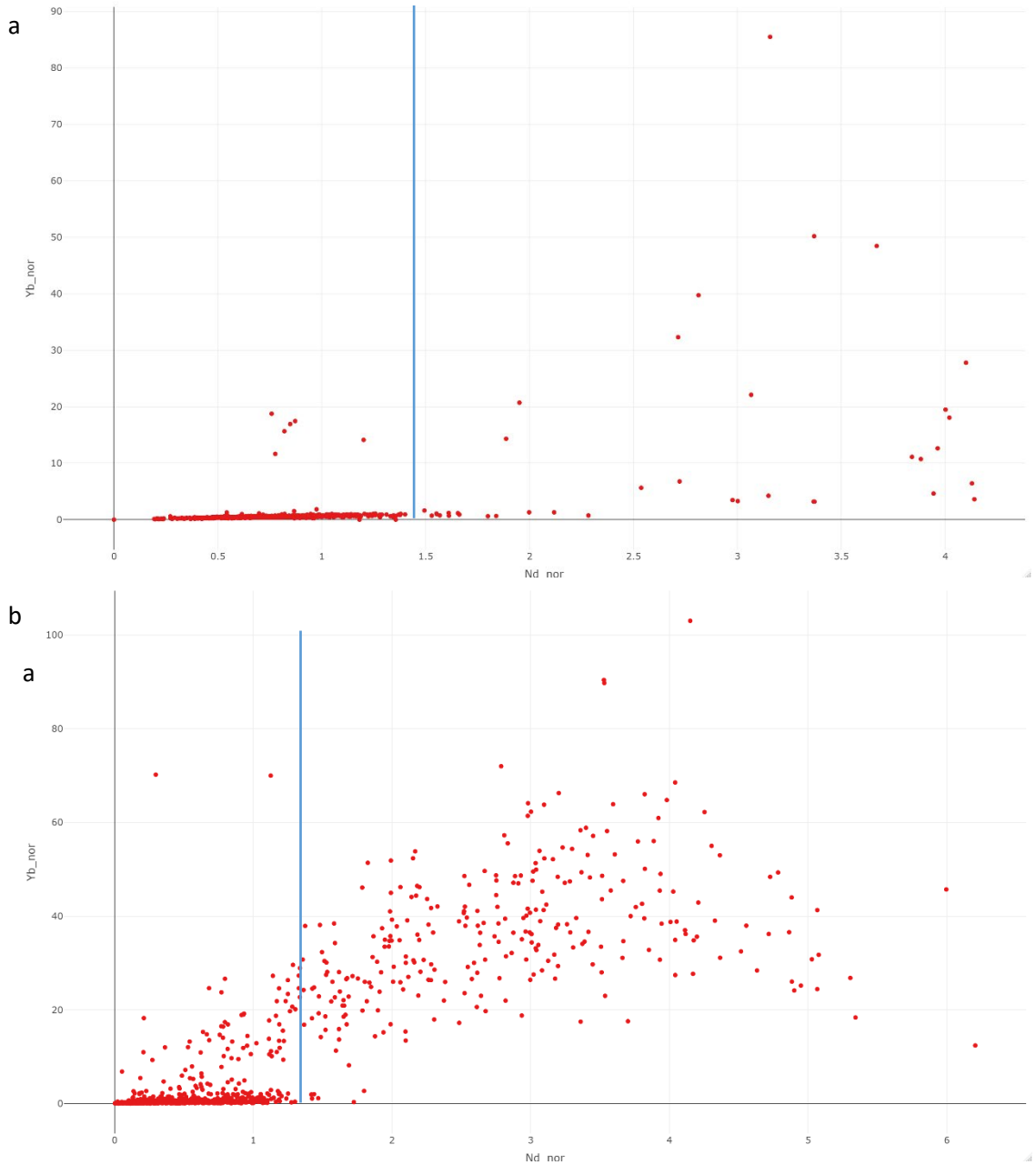

Figure 20: Point plots of the control (a) and taxol (b) sample where the normalized M-phase signal is plotted against the normalized G1·marker signal showing most cells which have a high G1-phase signal also have a high M-phase signal.

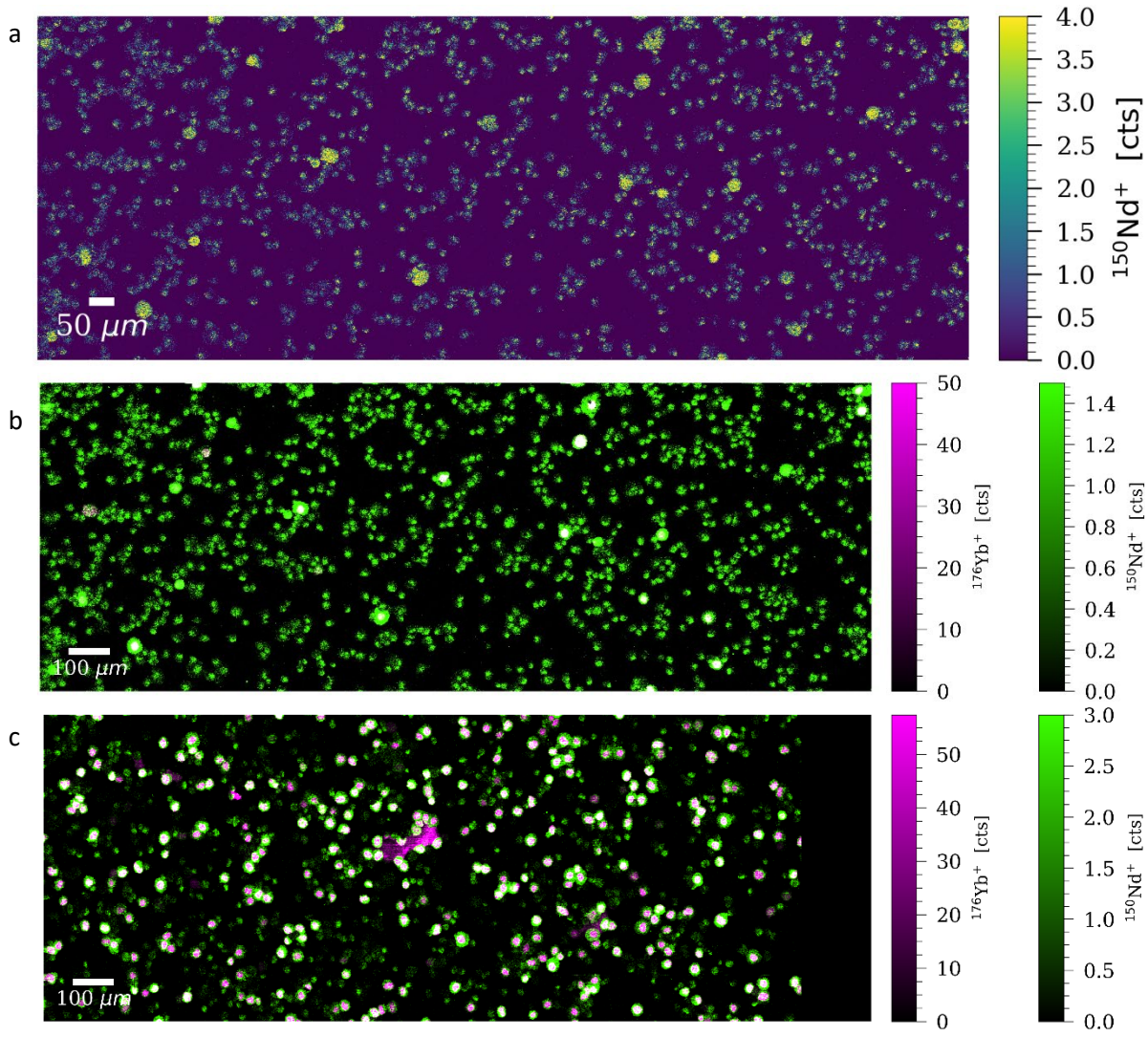

Figure 21: a: The ^{164}Dy-signal distribution within the HaCaT control sample showing that most cells contain the G1-phase marker whereas some cells are more intense. b: Overlap of the ^{164}Dy- and ^{176}Yb-signal within the HaCaT control sample showing that the cells shwoing the most G1 marker are cells within the M-phase. c: Overlap of the ^{164}Dy- and ^{176}Yb-signal within the HaCaT taxol treated sample showing that the cells shwoing the most G1 marker are cells within the M-phase.

When checking the overlap of the G1- and S-phase marker, all cells in S-phase show the G1-marker (Figure 22). Thus, all cells in the M- or S-phase show the G1-marker which is very unspecific. Especially when cells in the M-phase are the cells which give the most intense signals will lead to problems when thresholding. The two populations which can be seen in the point plots (Figure 20) are once cells in the M-phase (right side of the threshold) and the other population are cells in the G1-, G2- or S-phase (left side of the threshold). Thresholding is consequently not possible.

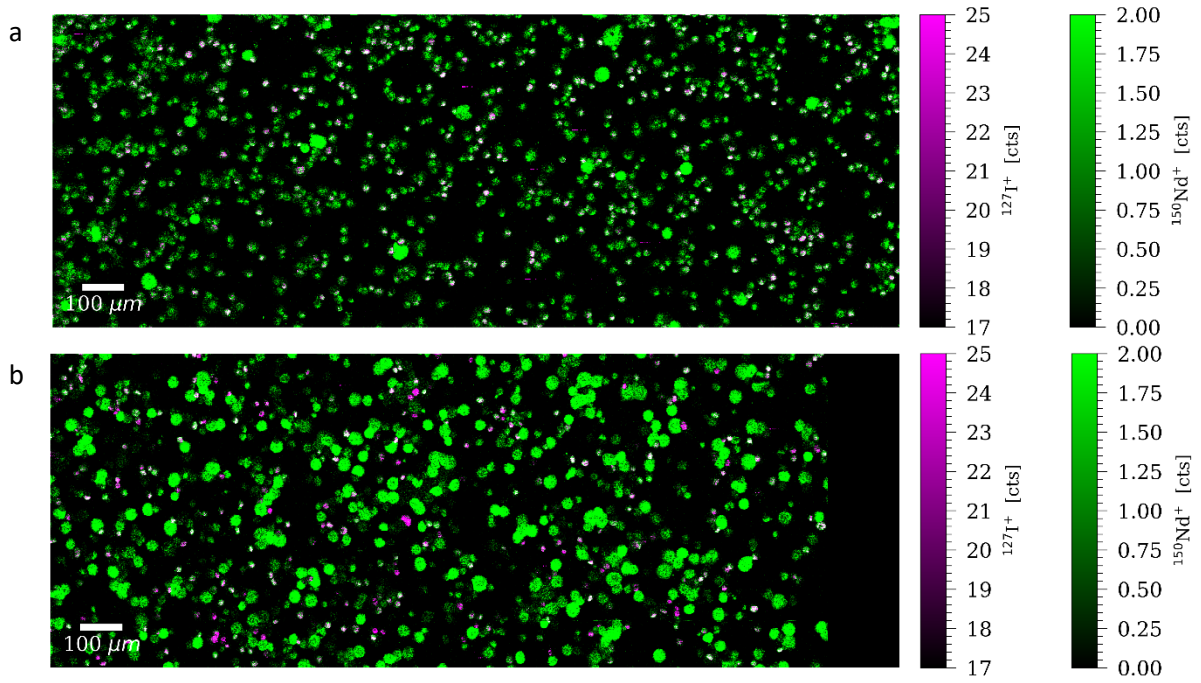

Figure 22: Overlap of the ^{127}I and ^{150}Nd signal within the HaCaT control (a) and taxol (b)sample showing an overlap of the G1- and S-phase marker. Cells in the S-phase thus show the pRb (G1)-marker. The bigger cells showing no ^{127}I-signal are cells in the M-phase which were described in chapter 4.2.4.

When it comes to the low intensity of the G1-marker within the cells, this might be again the case that signaling and regulating proteins are less abundant compared to structural and functional proteins like the histone and IdU marker which is heavily incorporated into the DNA.[50] Both markers might naturally come in higher concentrations compared to the pRb protein. The Rb-protein content in the cells continuously rises during the G1-phase until it reaches a peak in the late G1-phase and rapidly declines when phosphorylated as the phosphorylation changes its conformation and thus probably reduces the affinity to the antibody. The antibody is staining in special the pRb [S807/S811]. The unspecificity which we measure is also probably the reason, why Stokke et all could only stain the late G1-phase, and they used the pRb marker only for the differentiation between the early and late G1-phase. In their analysis, the pRb marker stained all the phases except for the early G1-phase and the M-phase was stained the most which is also true four our measurements.

As already stated, there are three possible reasons for why most of the cells show the G1-marker. All cells of all measurements and all treatments being in the G1-phase is very unlikely and does not fit the FACS data received from the Medical University of Vienna as well as the literature.[23] The FACS data will be discussed into depth in part 4.3.9.

Theoretically, the pRb [S807/S811] protein should not be present in all the cell cycle phases. However, unfunctional, disturbed or compromised proteins sometimes are not properly

degraded. On how far the pRb-protein is altered and if the antibody can still mark the possibly compromised pRb-protein is not known and can not be discussed without further investigation. Additionally, the pRb-protein is often compromised within tumor cells[47a] as it is also one cause for the formation of the development of tumor cells by increasing the genome instability.[47b] It can just be speculated that the A2780 cells contain such an altered or compromised pRb-protein. The HaCaT cells being immortalized healthy cells should theoretically have no altered pRb-protein. It is also not known, on how far the immortalization might influences the pRb-protein. One other possibility for why the pRb-protein is present throughout the cell cycle is that 13 phosphoylation patterns are known for the Rb-protein. Depending on which serine or threonine is phosphorylated, the conformation of the protein changes.[18] The antibodies for the actual anti-pRb [Ser807/811] protein might have a small affinity to the other conformations. However, this is just a speculation. Finally, the measured signals can also just come from unspecific binding and just overlap the low signal of the marker.

When speaking about the G1- and G2-phase marker, it must be considered, that both markers are made for liquid samples and not for solid samples. So, there is no staining process which can exactly be followed, and an optimization still must be done.

4.3.6 Optimization of the G1- and G2-marker staining processes

As previously explained, most of the cells show the G1 (^{150}Nd) or G2 (^{164}Dy) marker. This problem was tried to be solved by reducing the maker concentration from 1:50 to 1:200 at a staining temperature of 4 °C for 24 h (Optimization 1). The aim was, to reduce the available marker concentration in the cell to allow much less unspecific binding so that the cells being positive for the G1 and G2 marker are no longer overlapped by the high background signal due to too much unspecific binding. In a second attempt, the usual 1:50 marker dilution was used whereas the staining time was reduced to 30 minutes at room temperature for both markers (Optimization 2). Here, the aim was to have less time for unspecific binding to happen if this is time dependent. Both samples are HaCaT control samples which have been ablated with a spot size of 2 µm overlapping by half resulting in 1 µm spot sizes with a fluence of 1.3 J/cm^2. When looking at the raw data, no visual difference can be seen as many cells show a signal for the G2- and G1-marker.

For the point plots of the G1-marker (Appendix 5) there are again two separate populations which can be identified. However here are just a view cells showing high ^{150}Nd-signals and most of those cells are cells in the M-phase again compared to the non-optimized HaCaT control sample. Hence, neither of the two optimizations of the G1 marker was successful. Additionally, the intensities for the G2-marker for the two optimization attempts were lower compared to the HaCaT control sample. The first optimization showed higher ^{150}Nd-signals and the second optimization attempt showed lower ^{150}Nd-signals compared to non-optimized HaCaT control sample.

For the point plots of the G2-marker (Appendix 6 - Appendix 5) there are again no two distinct populations which can be identified but rather a transition gradient compared to the non-optimized HaCaT control sample. Many cells showing high ^{164}Dy-signals are cells in the M- or S-phase. Hence, neither of the two optimizations of the G1 marker was successful. Additionally, the intensities for the G2-marker for the two optimization attempts were lower compared to the non-optimized HaCaT control sample.

To conclude, none of the two optimization attempts was successful.

4.3.7 G0-phase

The evaluation of cells being in the G0 phase is rather difficult. There are three main possibilities, to assign the G0-cells. Firstly, cells showing none of the four cell cycle markers should theoretically be cells in the G0-phase or dead cells. The G1 and G2 marker being very unspecific up to now makes this rather difficult. Secondly, all proliferating cells should theoretically show a signal for ^{168}Er, the KI-67 protein or proliferation marker. However in the taxol sample, cells in the S-phase thus do not the proliferation marker whereas the control, cisplatin and 0% serum sample show the marker in all the cell cycle phases including the S-phase.

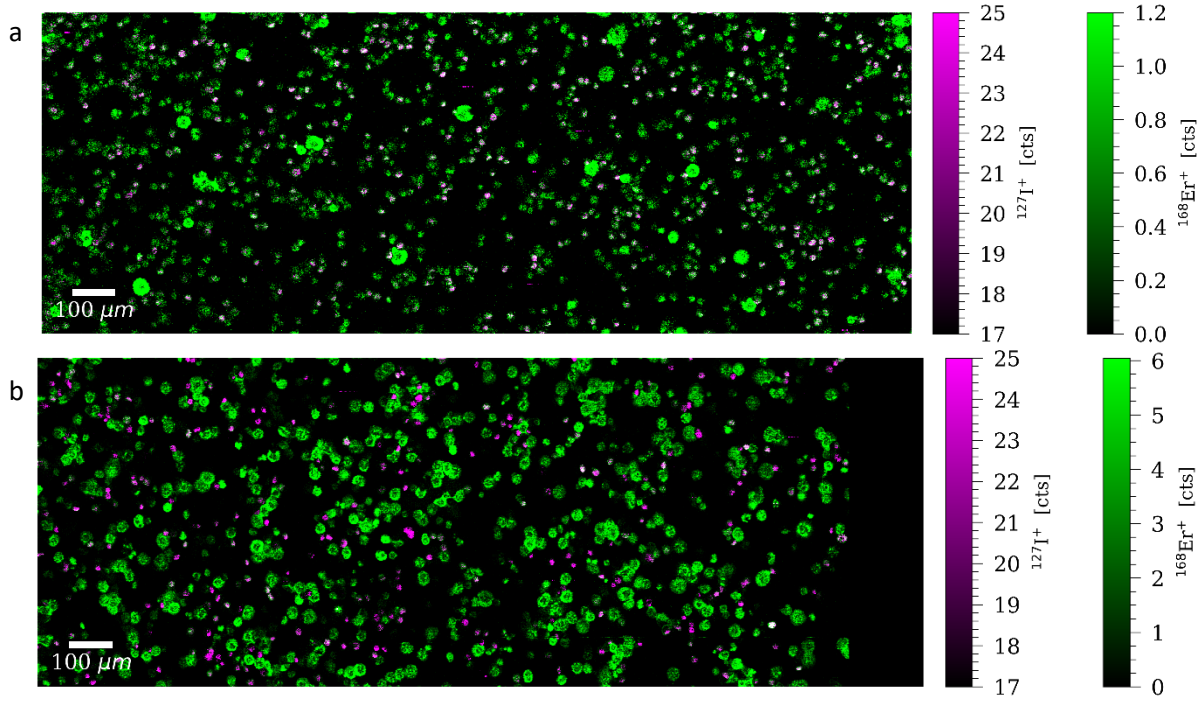

Figure 23: Overlap of the S-phase and proliferation marker for the control (a) and the taxol treated HaCaT sample.

The third possibility would be to stain a protein which is only present in ground state. To conclude, even if the determination of the cells in the G0 phase is not the main objective of this work but rather the determination of the cell cycle phases, the evaluation of the cells in the G0 is corrupted up to date. One possibility to determine the G0 phases not by the principle of exclosure but also to use a marker specific for the non-proliferating cells. If G0 cells could be attributed specifically like the S- and M-phase, a differentiation between non proliferating cells, cells in the M-phase, cells in the S-phase or the gap phase can be made.

4.3.8 Dead cells

Cells which died because of apoptosis or for a different reason can be differentiated from living cells under the microscope. If this information can be implemented into this work, it would be possible to track down dead cells which again would improve the differentiation between all the different phases. If a cell dies in the M phase and the histone proteins are still present, this cell would be assigned to being a cell in the M-phase whereas it is not anymore. Furthermore, dead cells might show more unspecific binding as everything in the cell is broken down which leads to many junk which is not present in living cell. The cells' membrane is broken down, proteins decompose as well as the DNA. Many proteins are expressed which lead to the cell death.[51]

During apoptosis, many proteins are expressed which are specific for the controlled cell death. By using a specific marker, cells which have undergone apoptosis can be tracked town. However, the method using the microscope would be less expensive and cells which have died because of a different reason than apoptosis. There is also the possibility to differentiate between living and dead cells by staining the cells before the fixation with a DNA-intercalator. For this a DNA-intercalator can be used with a different metal as ^{193}Ir. For such a live/dead staining, the Cell-ID Intercalator-^{103}Rh can be added after the treatment which has already been used for imaging mass cytometry.[52]

4.3.9 Comparison of the data with FACS-data as well as the mean area of the different cell cycle phases

The data can not really be compared to the received FACS Data because the FACS-measurement can not differentiate between the G2- and M-phase as the amount of nucleic acid content is tracked down which is the same in both phases (part 1). Thus, only the S-phase and G1-phase could be compared. The staining with the G1- and G2-phase marker is not completely optimized and both markers are not as specific as they could be. (See part 4.3.4 and 4.3.5) The following evaluation has been done based on the best knowledge for thresholding and it has to be kept in mind, that small changes in the thresholding for the G1 and G2 marker may lead to different results. As the markers show more specificity within the taxol treated sample, this one can be properly evaluated whereas the other treatments need to be evaluated with suspiciousness. The evaluation of the cell cycle distribution and comparison with the FACS-data is listed up in Table 9. The tables for the control, cisplatin and 0% serum

sample are listed in the appendix (Appendix 4) The thresholds four all the samples have been set individually as the signal intensities differ from sample to sample (see part 4.3.1) and the specificity of the G1 and G2 marker differ when cells are treated differently (part 4.3.4 and 4.3.5). The shares of the cell cycle phases for the measurement and FACS-data show the same trend and are in the same magnitude. The G1-phase being the smallest share with 1.1% for the taxol measurement and 10.6% for the FACS-data. The S-phase represents the second biggest share with 23.7% whereas 13.5% for the FACS-data and the S-phase marker is one of the two markers which seems to be very specific. When looking at the raw images from the LA-ICP-TOFMS, it also shows no overlap with the M-phase marker which is also more specific. The G2- and M-phase combined are the largest group for both measurements, the FACS-data (53.2%) and our measurement (44.5%). The share of the cells showing none of the markers are cells within the G0-phase or are dead cells. Tumor cells are known for being cells where the cell cycle homeostasis is disturbed. Thus, for cancer cells, the number of cells being in the G0-phase or dead should be rather low. However, the HaCaT cells are healthy immortalized cells which could explain the rather high number of cells being in a nonproliferation state. The aim of the treatments was to arrest the cells in one of the proliferation states. When cells growing in a monolayer become 100% confluent, they might undergo a density arrest.[53] As described in part 3.2, the HaCaT cell culture was to dense in order to treat them. Because of the risk of the cells having begun the density arrest, the cells have been recultivated and were treated only 3 hours after recultivation. This was done by the Medical University of Vienna. With, 11.4 % for the 0% serum and 83.2 % for the cisplatin sample our measurements are comparable to the FACS-data showing 7.6 % for the 0% serum and 69.5 % for the cisplatin treated sample when it comes to the attribution of the S-phase. Only the control sample shows approximately twice as many cells in the S-phase for our measurements (48.3 %) compared to the data from the Medical University of Vienna (24.8 %).

For the G1-phase, all measurements show less cells in the G1-phase compared to the FACS-data. Especially the 0% serum sample which should arrest most cells in the G1-phase only shows a share of 9.7 % for our measurements whereas 69.5 % for the FACS measurements. This again shows that the G1-marker staining must be optimized. To conclude, the cell cycle arrests have worked according to the FACS-data. The distribution of the cell cycle phases according to literature corresponds to the actual measurements of the FACS-data and to the measurements via LA-ICP-TOFMS for the S- and M-phase. According to literature, the sample treated with taxol arrest the cells in the M-phase. The taxol treated sample also shows

from all the samples the most cells in the M-phase with 33 % compared to the control sample with 2.9 %, the cisplatin treated sample with 0.4 % and 0.7 % for the 0% serum sample.

The cell cycle arrest for the taxol and cisplatin treated sample were successful as more of the cells are in the desired cell cycle phase. For the 0% serum sample, the cell cycle arrest in the G1-phase was successful according to the FACS-data but can not bet affirmed by our measurements yet.

Table 9: Listing of the thresholds set for the four cell cycle phases as well as the cells detected, the mean area of the cells, the share of cells within the measurement of the taxol sample and the FACS data received.

Taxol:	Threshold [cps/area]	Cells detected	share [%]	FACS data [%]	Mean number of pixels per cell
G1	1.2	2	0.2	10.6	253
S	11.5	306	25.7	13.5	520
G2	0.2	106	10.6	53.2	540
M	2	393	33		644
G0/A	/	365	30.7	22.7	444

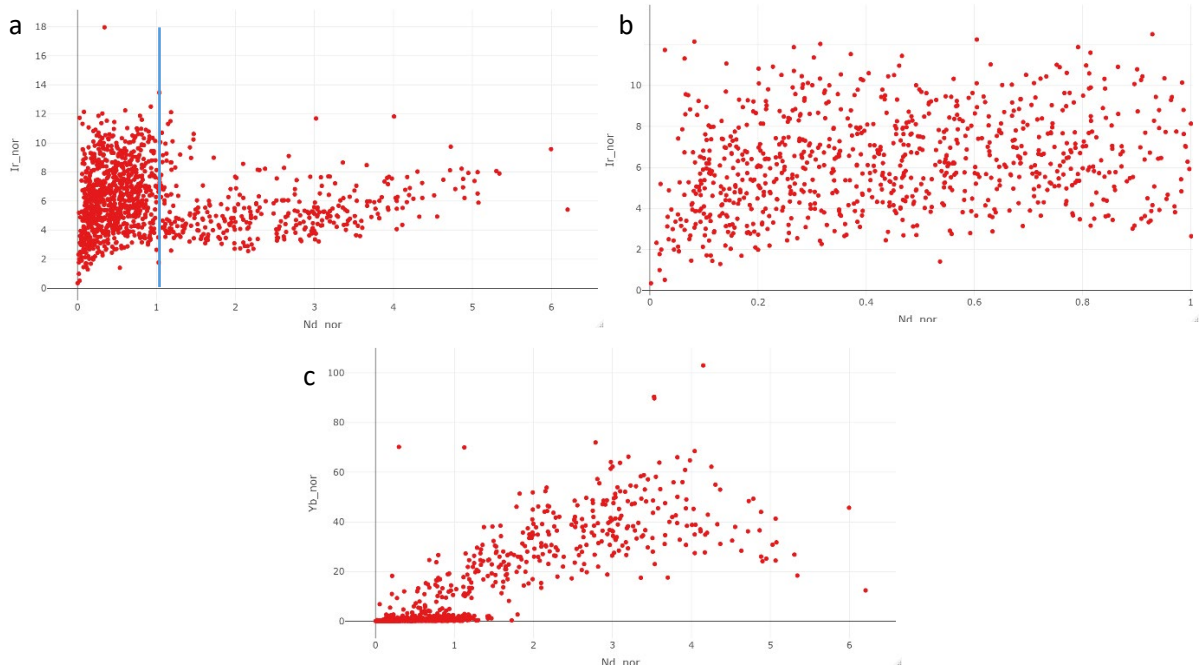

Figure 24: Point plots of the normalized G1-marker signal (^{150}Nd) plotted against the normalized DNA-intercallator signal (^{193}Ir) (a), a zoomed in version (b) and plotted against the normalized M-marker signal (^{176}Yb). The sample used for this data is the taxol treated sample.

For the thresholding of the G1-phase marker, it seems like the setting of the thresholding is rather simple because two different populations can be identified. In a first glance, the threshold would be set at a signal intensity of 1 CPS/pixel (Figure 24a). However, when plotting the ^{150}Nd-signal (G1-marker) against the ^{176}Yb-signal (M-marker), it is obvious, that all cells higher

than the threshold set previously are cells within the M-phase (Figure 24c). These cells should thus be excluded from the data for the determination of the cells in the G1-phase. For the remaining cells, it can not be differentiated between two or more populations (Figure 24b) and no threshold could be set. Thus, the threshold of 1 CPS/pixel was taken for the evaluation.

During the cell cycle, the cells dimension grows to two daughter cells that are fully functional.[10] This growth of the cell can also be observed by comparing the mean area of the cells of the different cell cycle phases. Cells in the G1-phase are on average the smallest cells with 338 pixels, followed by the S-phase and G2-phase with 520 and 542 pixels and the M-phase with an average of 644 pixels per cell. The cell dimension thus grows over the course of the cell cycle as described in literature.[41] This was true for the taxol, control and cisplatin treated sample. For the 0% serum sample, the G2-phase (364 pixel per cell) was noticeably smaller compared to the cells in the S-phase (515 pixels per cell).

5 Summary and Outlook

5.1 Summary

The aim of the work was the development of a staining procedure of the four cell cycle phases in order to analyze via LA-ICP-TOFMS the distribution of the cell cycle phases within different cell cultures (A2780 and HaCaT). Problems like segmentation of too dense cytospins or a too high ^{127}I-background signal could be solved by making less dense cytospins and using different segmentation methods or by changing the incubation time of the cell culture with IDU. From the different segmentation methods tested, cellpose showed the best results as it uses two combined signals (^{63}Cu and ^{193}Ir) for the segmentation. When the segmentation algorithm is trained, cellpose also represents the fastest method with the possibility to manually redraw cells when mismatches or duplicates occur. The M- and S-phase marker show a high specificity when tagging the respective phase. The share of cells within the S-phase is in the same order of magnitude for the four treatments compared to the FACS data from the Medical University of Vienna. The share of cells within the M-phase can not be compared as the FACS-measurement can not differentiate between the M- and the G2-phase. If different fluorescence markers had been used, this is also possible by flow cytometry. The G1- and G2-phase markers show insufficient results. There is no staining procedure available for both markers for solid samples as they are both liquid markers. Their staining procedure must be optimized yet or other proteins might be traced down. Strangely, G2 marker showes a different specificity for the different treated samples. Here, further measurements must be made. Thresholding is still improvable as for some markers (G1 and G2), the setting of the threshold is very subjective because there is a smooth transition in the signal intensity between cells in different cell cycle phases or the cells showing the most intense G1- or G2-marker signal are cells in the M- or S-phase leading to the wrong placement of the thresholds.

To conclude, up to now, it can be differentiated between three groups. Cells being in the S-phase, cells being in the M-phase or cells being in one of the G-phases (G0, G1 or G2).

5.2 Outlook

In this thesis, cell cycle assessment by imaging mass cytometry was scrutinized – considering all relevant aspects of the workflow from sample preparation to selectively, labelling the individual cell cycle phases and finally to automatized image analysis. In fact, data evaluation in imaging requires accurate and automatized cell segmentation strategies. Statistical analysis should consider a considerably study size in the range of 1000s of individual cells, thus a manually curated cell integration is precluded. The workflow establishment was based on cytospin preparations as they provide ideal case scenarios with well separated cells deposited on surfaces. While cell segmentation and automatized image analysis was successfully established, selective labelling of all cell cycles, which seemed to be a straightforward task, on the contrary turned out to be challenging. These lacking selectivity led to the situation that not all cell cycle phases could be assessed accurately. Further studies will be needed.

6 Sources

[1] I. Vitale, E. Shema, S. Loi, L. Galluzzi, *Nat Med* **2021**, *27*, 224.
[2] A. C. Bakke, *Laboratory medicine* **2001**, *32*, 211.
[3] J. Flores-Montero, T. Kalina, A. Corral-Mateos, L. Sanoja-Flores, M. PГ©rez-AndrГ©s, M. Martin-Ayuso, L. Sedek, K. Rejlova, A. Mayado, P. FernГЎndez, V. van der Velden, S. Bottcher, J. J. M. van Dongen, A. Orfao, *J Immunol Methods* **2019**, *475*, 112618.
[4] G. K. Behbehani, S. C. Bendall, M. R. Clutter, W. J. Fantl, G. P. Nolan, *Cytometry A* **2012**, *81A*, 566.
[5] I. D. Rein, H. Ø. Notø, M. Bostad, K. Huse, T. Stokke, *Cytometry A* **2020**, *97*, 844.
[6] M. E. Ijsselsteijn, R. van der Breggen, A. F. Sarasqueta, F. Koning, N. F. C. C. de Miranda, *Front Immunol* **2019**, *10*, 2534.
[7] Y. Zhou, H. Li, H. Sun, *Chem Commun (Camb)* **2017**, *53*, 2973.
[8] C. J. Sherr, *Science* **1996**, *274*, 1677.
[9] L. Ding, J. Cao, W. Lin, H. Chen, X. Xiong, H. Ao, M. Yu, J. Lin, Q. Cui, *Int J Mol Sci* **2020**, *21*.
[10] E. D. Israels, L. G. Israels, *The Oncologist* **2000**, *5*, 510-513.
[11] R. Suryadinata, M. Sadowski, B. Sarcevic, *Bioscience reports* **2010**, *30*, 243-255.
[12] M. B. Kastan, S. J. Kuerbitz, *Environ Health Perspect* **1993**, *101 Suppl 5*, 58.
[13] J. W. Harbour, R. X. Luo, A. D. Santi, A. A. Postigo, D. C. Dean, *Cell* **1999**, *98*, 869.
[14] C. Bertoli, J. M. Skotheim, R. A. M. de Bruin, *Nat Rev Mol Cell Biol* **2013**, *14*, 528.
[15] C. Giacinti, A. Giordano, *Oncogene* **2006**, *25*, 5220.
[16] K. MГjnger, P. M. Howley, *Virus Res* **2002**, *89*, 228.
[17] B. E. Engel, W. D. Cress, P. G. Santiago-Cardona, *Cell Health Cytoskelet* **2015**, *7*, 1-10.
[18] S. M. Rubin, *Trends Biochem Sci* **2013**, *38*, 19.
[19] T. Waldman, K. W. Kinzler, B. Vogelstein, *Cancer Res* **1995**, *55*, 5190.
[20] H. Murad, M. Hawat, A. Ekhtiar, A. AlJapawe, A. Abbas, H. Darwish, O. Sbenati, A. Ghannam, *Cancer Cell Int* **2016**, *16*, 39.
[21] S. Dasari, P. B. Tchounwou, *Eur J Pharmacol* **2014**, *740*, 364-378.
[22] D. J. Beck, R. R. Brubaker, *Journal of Bacteriology* **1973**, *116*, 1247-1252.
[23] F. Un, *Anticancer Drugs* **2007**, *18*, 411-417.
[24] M. Kielbik, D. Krzyzanowski, B. Pawlik, M. Klink, *Oncotarget* **2018**, *9*, 19847-19860.
[25] Y. H. Choi, Y. H. Yoo, *Oncol Rep* **2012**, *28*, 2169.
[26] M. Segurado, J. A. Tercero, *Biol Cell* **2009**, *101*, 627.
[27] V. Oakes, W. Wang, B. Harrington, W. J. Lee, H. Beamish, K. M. Chia, A. Pinder, H. Goto, M. Inagaki, S. Pavey, B. Gabrielli, *Cell Cycle* **2014**, *13*, 3311.
[28] G. R. Stark, W. R. Taylor, *Mol Biotechnol* **2006**, *32*, 248.
[29] J. Kalous, D. JansovГЎ, A. E uEЎor, *Cells* **2020**, *9*.
[30] D. Gong, J. E. Ferrell Jr, *Mol Biol Cell* **2010**, *21*, 3161.
[31] aO. Gavet, J. Pines, *J Cell Biol* **2010**, *189*, 259; bJ. Pines, T. Hunter, *J Cell Biol* **1991**, *115*, 17; cP. S. Frisa, J. W. Jacobberger, *PLoS One* **2009**, *4*, e7064.
[32] K. J. Barnum, M. J. O'Connell, *Methods Mol Biol* **2014**, *1170*, 29-40.
[33] T. Scholzen, J. Gerdes, *J. Cell. Physiol* **2000**, *182*, 322.
[34] J. Gerdes, H. Lemke, H. Baisch, H. H. Wacker, U. Schwab, H. Stein, *J Immunol* **1984**, *133*, 1710-1715.
[35] X. Sun, P. D. Kaufman, *Chromosoma* **2018**, *127*, 186.
[36] F. Hans, S. Dimitrov, *Oncogene* **2001**, *20*, 3027.
[37] S. Dhara, *Indian J Chem* **1970**, *8*, 193-194.
[38] C. Stringer, T. Wang, M. Michaelos, M. Pachitariu, *Nat Methods* **2021**, *18*, 106.
[39] M. Pachitariu, C. Stringer, *Nature methods* **2022**.
[40] S. J. M. Van Malderen, T. Van Acker, F. Vanhaecke, *Anal. Chem* **2020**, *92*, 5764.
[41] C. Cadart, L. Venkova, M. Piel, M. Cosentino Lagomarsino, *Elife* **2022**, *11*.
[42] H. Tsuiki, M. Nitta, M. Tada, M. Inagaki, Y. Ushio, H. Saya, *Oncogene* **2001**, *20*, 429.

[43] S. Theiner, A. Schweikert, C. Haberler, A. Peyrl, G. Koellensperger, *Metallomics* **2020**, *12*, 1252.
[44] aL. Cortes, B. R. Roberts, A. G. Wedd, Z. Xiao, *Inorg. Chem* **2017**, *56*, 5284; bS. Osaki, D. A. Johnson, E. Frieden, *J Biol Chem* **1966**, *241*, 2751.
[45] R. Hänsch, R. R. Mendel, *Current Opinion in Plant Biology* **2009**, *12*, 259-266.
[46] A. J. Herrmann, S. Techritz, N. Jakubowski, A. Haase, A. Luch, U. Panne, L. Mueller, *Analyst* **2017**, *142*, 1710.
[47] aA. Doan, J. Arand, D. Gong, A. P. Drainas, Y. T. Shue, M. C. Lee, S. Zhang, D. M. Walter, A. C. Chaikovsky, D. M. Feldser, H. Vogel, L. E. Dow, J. M. Skotheim, J. Sage, *PLoS Genet* **2021**, *17*, e1009941; bR. VΓ©lez-Cruz, S. Manickavinayaham, A. K. Biswas, R. W. Clary, T. Premkumar, F. Cole, D. G. Johnson, *Genes Dev* **2016**, *30*, 2512.
[48] D. Hanahan, RobertB A. Weinberg, *Cell* **2011**, *144*, 674.
[49] M. Bortolomeazzi, L. Montorsi, D. Temelkovski, M. R. Keddar, A. Acha-Sagredo, M. J. Pitcher, G. Basso, L. Laghi, M. Rodriguez-Justo, J. Spencer, F. D. Ciccarelli, *Nat Commun* **2022**, *13*, 781.
[50] M. Beck, A. Schmidt, J. Malmstroem, M. Claassen, A. Ori, A. Szymborska, F. Herzog, O. Rinner, J. Ellenberg, R. Aebersold, *Mol Syst Biol* **2011**, *7*, n/a.
[51] V. Papaliagkas, A. Anogianaki, G. Anogianakis, G. Ilonidis, *Hippokratia* **2007**, *11*, 113.
[52] A. Schoeberl, M. Gutmann, S. Theiner, M. Schaier, A. Schweikert, W. Berger, G. Koellensperger, *Anal. Chem* **2021**, *93*, 16465.
[53] G. Gradl, D. Faust, F. Oesch, R. J. Wieser, *Curr Biol* **1995**, *5*, 535.

7 Appendix

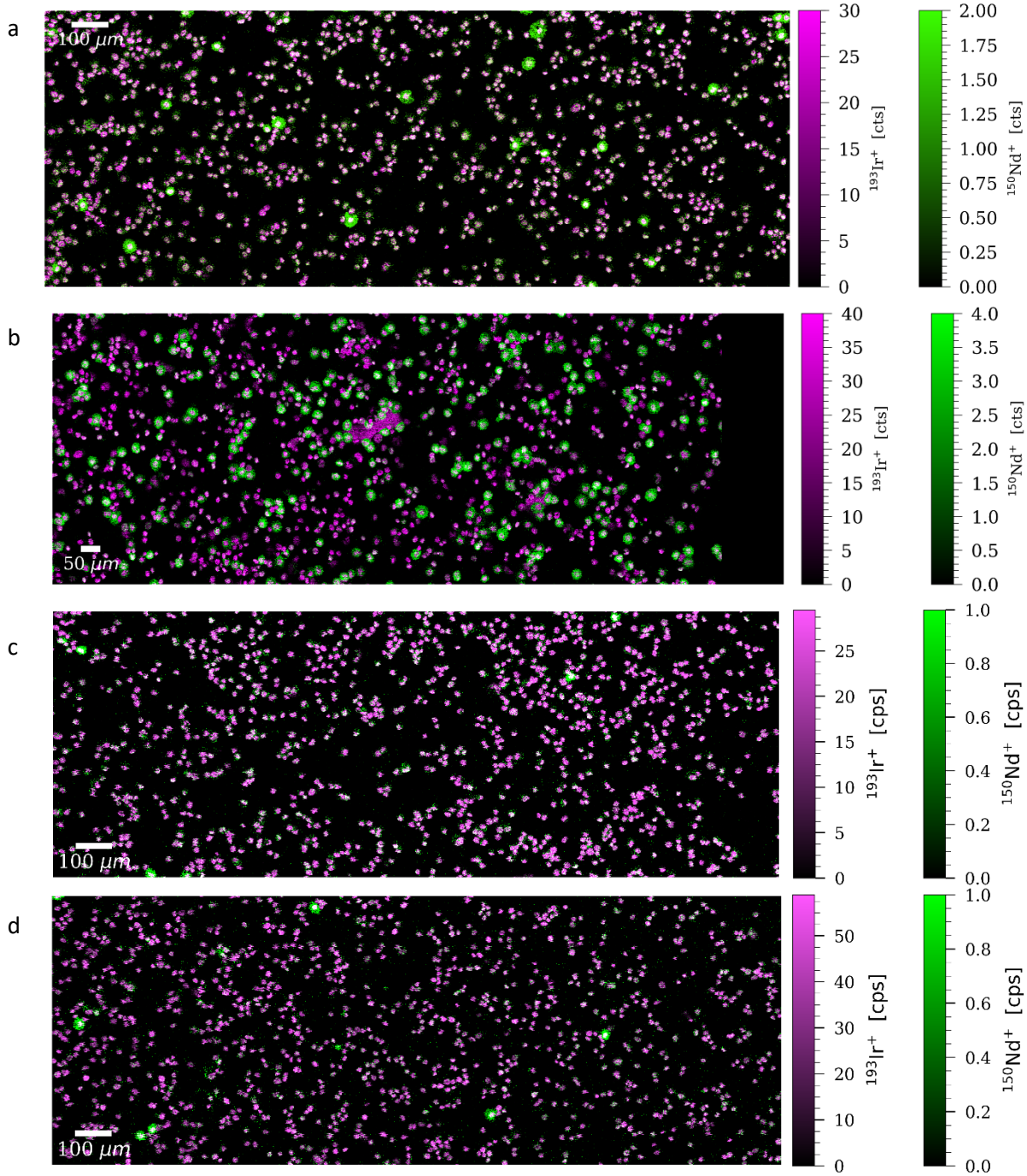

Appendix 1: Overlaps of the ^{150}Nd- and ^{193}Ir-signal for the comparison of the G1 marker distribution within the HaCaT samples. a: control sample; b: taxol treated sample; c: cisplatin treated sample; d: 0% serum sample.

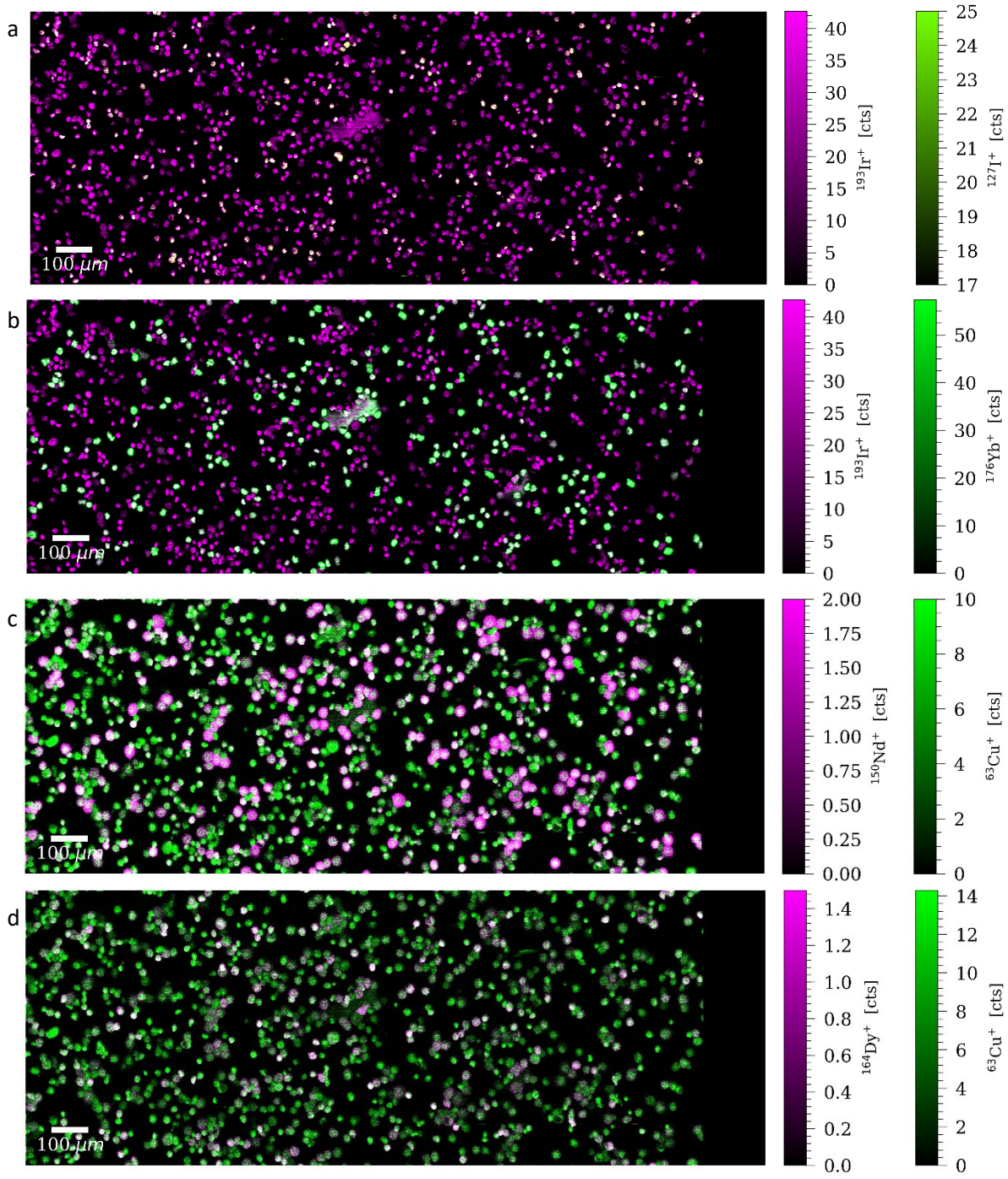

Appendix 2: Overlap of the ^{127}I- and ^{176}Yb-signal with the ^{193}Ir signal and overlap of the ^{150}Nd- and ^{164}Dy with the ^{63}Cu signal for the taxol treated sample to show that the G1- and G2-phase marker are distributed in the complete cell whereas the S- and M- phase marker are located within the nucelus.

a

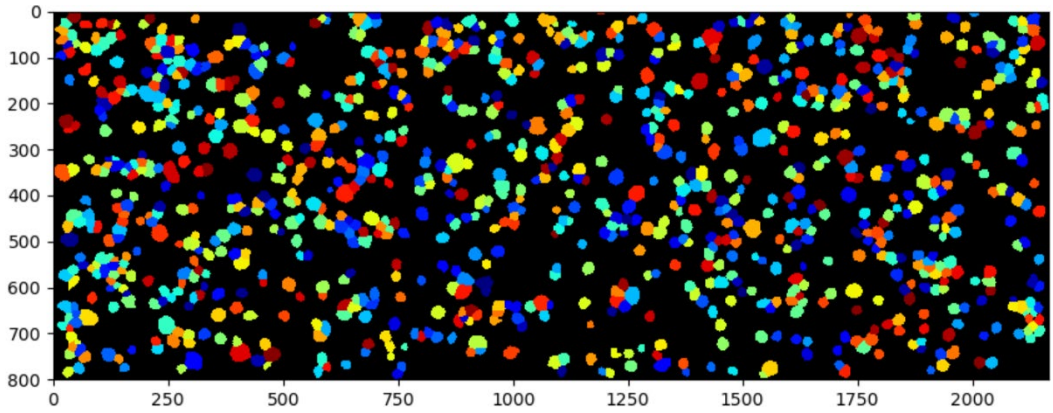

b

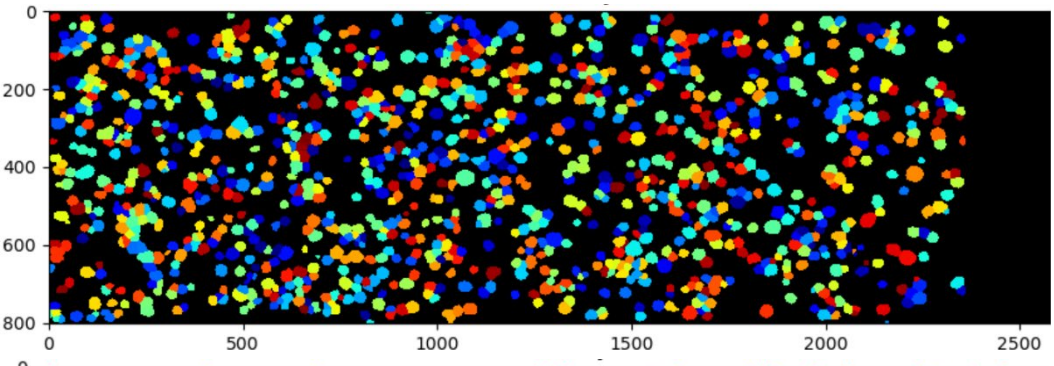

c

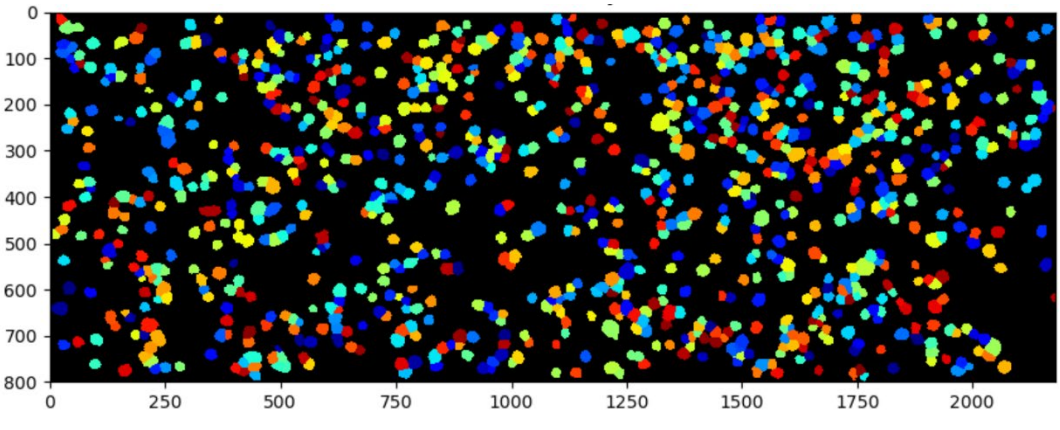

d

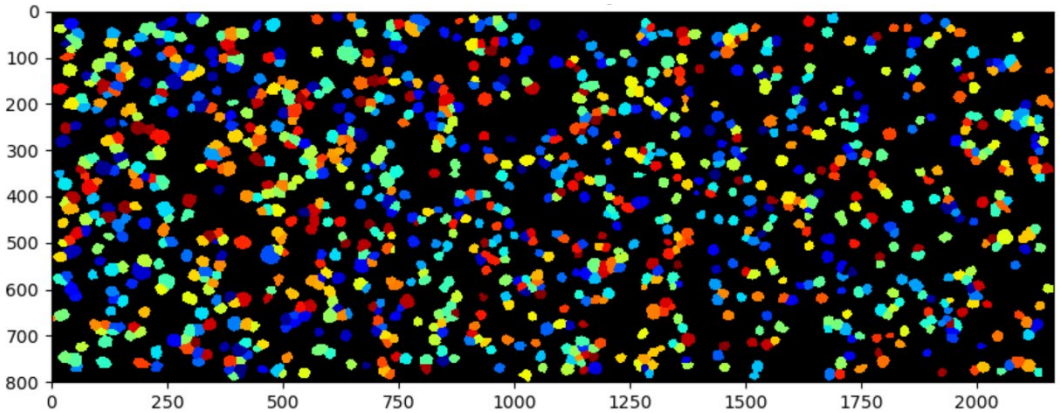

Appendix 3: Segmentation masks from cellpose which have been transferred to CellProfiler for the better visualization. All samples are HaCaT samples. a: control; b: taxol; c: cisplatin; d: 0% serum

Control:	Threshold [CPS/pixel]	Cells detected	share [%]	FACS data [%]	Mean number of pixels per cell
G1	1.3	11	1.1	30.1	321
S	11.5	505	48.3	24.8	477
G2	0.55	56	5.4	25.1	479
M	2	30	2.9		655
G0/A	/	444	42.4	20	416
Cisplatin:	**Threshold [CPS/pixel]**	**Cells detected**	**share [%]**	**FACS data [%]**	**Mean number of pixels per cell**
G1	0.25	36	3.5	13.7	415
S	12.5	860	83.2	69.5	436
G2	0.4	65	6.3	0	461
M	2	4	0.4		538
G0/A	/	69	6.7	16.8	485
0% Serum	**Threshold [CPS/pixel]**	**Cells detected**	**share [%]**	**FACS data [%]**	**Mean number of pixels per cell**
G1	0.2	11	9.7	62.4	346
S	15.5	130	11.4	7.6	515
G2	0.1	128	11.2	15.3	364
M	2	8	0.7		700
G0/A	/	764	67.0	14.7	398

Appendix 4: Listing of the thresholds set for the four cell cycle phases as well as the cells detected, the mean area of the cells, the share of cells within the measurement of the cisplatin, control and 0% serum sample as well as the FACS data received.

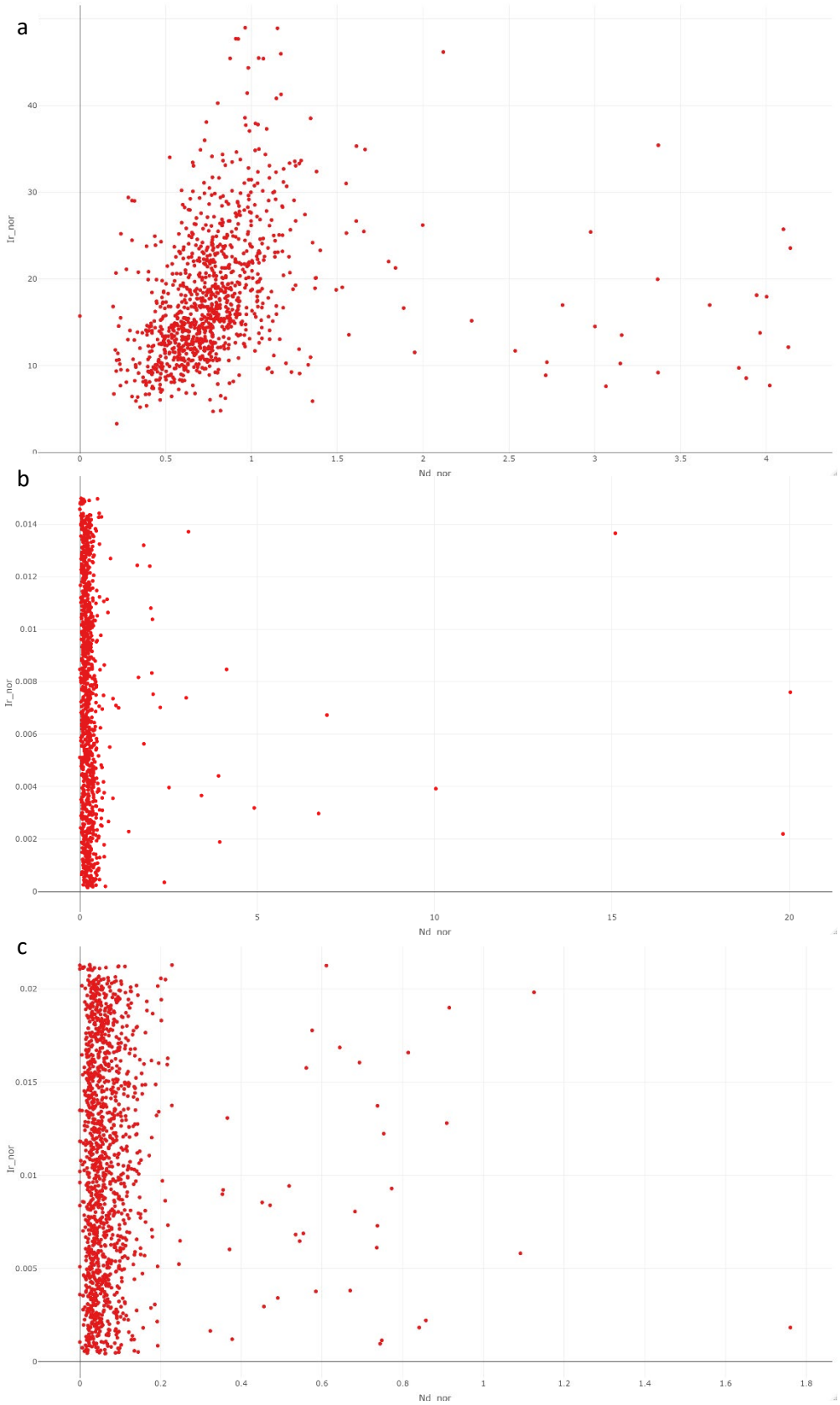

Appendix 5: point plots of the normalized G1 marker intensity vs the normalized ^{193}Ir-signal intensity for the control HaCaT sample from four main sample (a), for the Opti1 control sample (b) and for the Opti2 control sample (c).

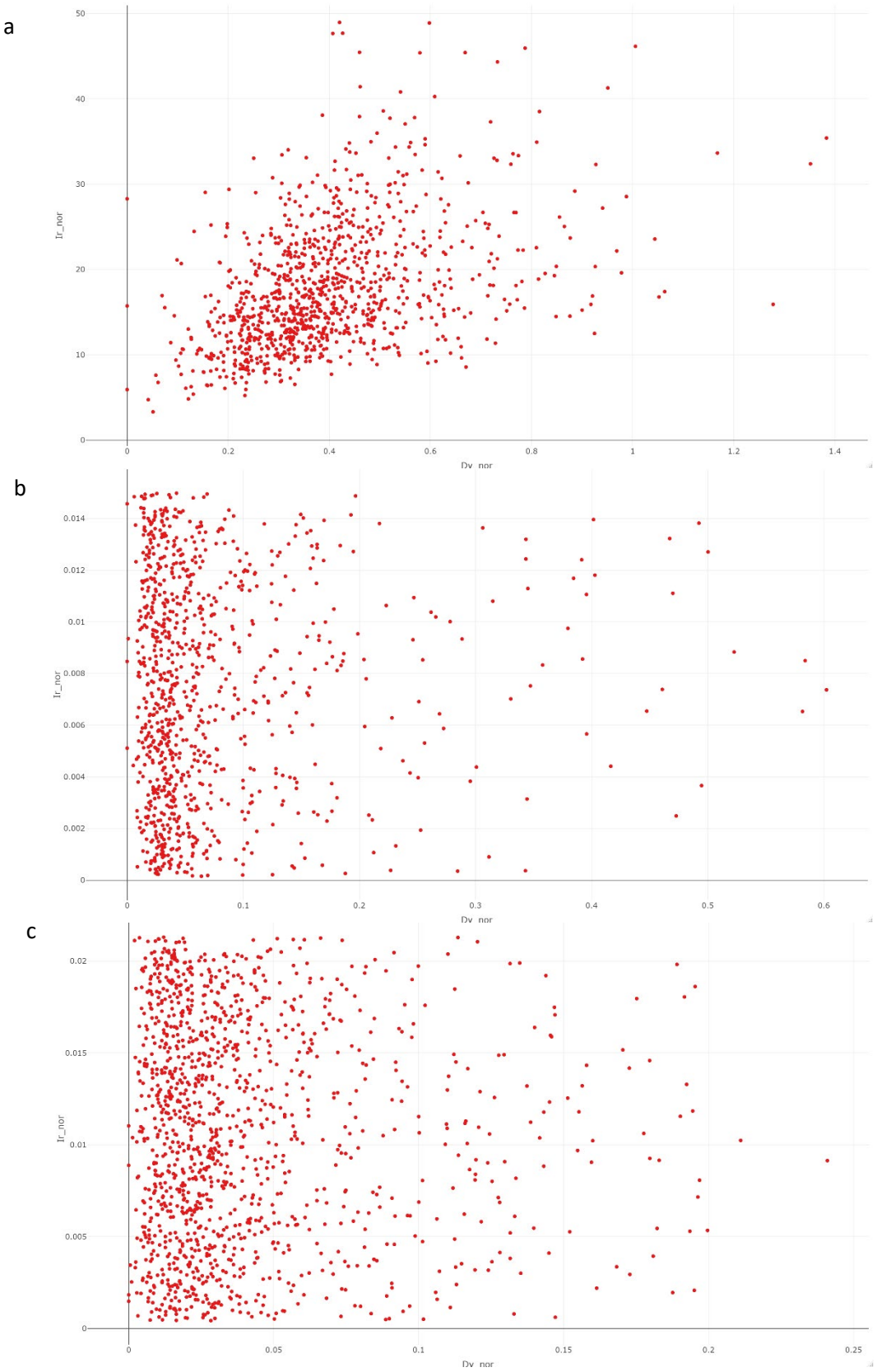

Appendix 6: point plots of the normalized G2 marker intensity vs the normalized ^{193}Ir-signal intensity for the control HaCaT sample from four main sample (a), for the Opti1 control sample (b) and for the Opti2 control sample (c).